

DRAFT | Peer Review Purposes Only | Not for Citation

Spring-run Chinook Salmon Juvenile Production Model

Authors

Josh Korman, Ecometric Research; Ashley Vizek, FlowWest; Liz Stebbins, FlowWest; Noble Hendrix, QEDA Consulting; Brett Harvey, California Department of Water Resources

Acknowledgments

The data used in this modeling effort are rich and extensive—in some cases, data collection has been ongoing since the late 1990s. This work would not be possible without the field staff collecting daily rotary screw trap data and the data stewards that have managed these data over time. Special thanks to the following individuals for running programs and synthesizing data for the Juvenile Production Estimate Modeling Team: Jason Kindopp, Feather River; Kassie Hickey, Feather River; Ryan Revnak, Mill and Deer Creek; Casey Campos, Yuba River; Mike Shraml, Battle and Clear Creek; Natasha Wingerter, Battle and Clear Creek; Grant Henley, Butte Creek.

We also thank the Spring-run Juvenile Production Estimate Core Team, Modeling Advisory Team, and Interagency Review Team for their useful comments and advice.

Work by Ecometric Research and FlowWest on this project was supported by California Department of Water Resources. Work by QEDA Consulting was supported by the California State Water Contractors organization.

Executive Summary

We developed a model, srJPE, that integrates a set of submodels to forecast abundance and timing of outmigrating juvenile spring-run Chinook salmon (*Oncorhynchus tshawytscha*) (spring-run) at the Sacramento–San Joaquin River Delta (Delta) entry to support development of potential measures to protect spring-run from operations of State and federal water projects, and to support development of other potential conservation actions. srJPE integrates predictions from three submodels:

- **A stock-recruit model** that forecasts annual outmigration abundance at rotary screw traps (RSTs) in spring-run tributaries based on the abundance of spawners and physical covariates (flow, water temperature, or discrete variables) in a forecast year (described in Chapter 7).
- **An inseason model** that uses estimates of cumulative abundance from the start of juvenile migration through a forecast week in a forecast year, and a forecast of the cumulative proportion of the juvenile run that has passed the traps by that week, to forecast annual outmigration abundance (described in Chapter 8).
- **A Cormack-Jolly-Seber (CJS) juvenile survival and travel time model** to forecast survival rates from RST locations to Delta entry (described in Chapter 9).

These submodels were fit to historical data to estimate posterior distributions of model parameters, and they were then used in srJPE to make forecasts of juvenile abundance and timing at RST sites and at Delta entry.

To demonstrate the behavior of srJPE, we used historical data to calculate inputs for a theoretical forecast year. srJPE was applied to data from six tributaries (Battle, Clear, Mill, Deer, Butte creeks, and Yuba River), and will eventually include data from Feather River when supporting models and estimates of spring-run outmigrant abundance are available. Chapters 4 and 5 describe how tributary and mainstem outmigrant abundance was modeled from RST catch data, and Chapter 6 describes how probabilistic length-at-date (PLAD) models were used to assign run identification to estimate spring-run-specific outmigrant abundance. As the migration season progresses and more information about abundance at RST sites from the inseason model becomes available, the precision of forecasts of outmigrating juvenile abundance at RST sites and at Delta entry increase from an early forecast date on December 28 to a later forecast date on March 29. Predictions of abundance at RST sites from the stock-recruit models were generally very uncertain, but did contribute prior information for srJPE forecasts early in the migration season when there was little information to estimate abundance from the inseason model.

Outmigrant abundance summed across RST sites was dominated by predictions from the Butte Creek and especially Yuba River RST sites owing to the substantively higher juvenile production in these tributaries. The spring-run juvenile abundance estimates at the Yuba River site are likely substantially overestimated and were excluded from further analysis in this chapter. Run identification predictions from the PLAD model for the Yuba River site require further examination as the model may be overestimating spring-run proportions as occurred at the lower Clear Creek RST site during earlier iterations of the Clear Creek models. The median estimate of abundance across tributary RST sites on the latest forecast date we evaluated (March 29) was 2.8 million fish with an 80% credible interval of 2.3–3.3 million fish (excluding the biased contribution from the Yuba River). The median estimate of abundance at Delta entry on the latest forecast date was 0.48 million fish with an 80% credible interval of 0.15–2.3 million fish. The ratio of median estimates of abundance at Delta entry to abundance at RST sites was 0.17. This ratio represents the RST abundance-weighted average of forecasted survival rates from RSTs to Delta entry in a forecast year with average flows during the outmigration period.

There was substantial uncertainty in forecasts of survival rate from RST locations to Delta entry, leading to higher uncertainty in forecasted abundance at Delta entry compared to the sum of abundances across RST sites. The coefficient of variation (CV) of the posterior distribution of sum of abundance estimates across tributary RST sites (Yuba Creek excluded) decreased from 1.02 to 0.11 between the first (December 28) and last (March 29) forecast dates. This difference was driven by the substantively reduced uncertainty in inseason estimates of abundance for later forecast dates especially for Butte Creek, which dominated the total abundance estimate. The CVs of posterior distributions of abundance at Delta entry also declined with later forecast date (1.52 on December 28 to 0.5 on March 29).

srJPE provides a robust approach to forecast spring-run juvenile abundance at Delta entry by combining information from submodels predicting juvenile outmigrant abundance at RST sites (stock-recruit, inseason), and from the survival submodel predicting survival rates from RSTs to Delta entry. One key advantage of srJPE is that it does not require a decision on when to switch from using a pre-season stock-recruit to an inseason approach for forecasting abundance at RST sites. Such decisions would be difficult because the amount of information about annual abundance at RST sites from these two sources varies across tributaries, and across forecast weeks within tributaries for the inseason model. srJPE provides a repeatable approach for blending information and will produce more precise JPEs because it maximizes the use of available information.

This chapter demonstrates how srJPE works, and is not intended to provide definitive JPE forecasts. Estimates of juvenile outmigration abundance at RST sites and Delta entry presented here should be considered preliminary owing to a number of issues such as bias in Yuba juvenile estimates, and Feather River data not included to date. To increase confidence in JPE forecasts, predictions from srJPE

and its submodels should be tested using out-of-sample data. These tests may reveal model limitations and ways to improve predictions.

srJPE also provides a pre-season estimate of arrival timing of spring-run juveniles in the Delta for populations from different tributaries, and for the aggregate population. In mixed-stock salmon fisheries, populations of different productivities or abundances are exposed to the same fisheries, and this information on tributary-specific outmigration timing could be used to tailor protections for more sensitive stocks.

The date when 50% of spring-run outmigrants arrived in the Delta varied considerably across tributaries. Clear Creek had the earliest median timing (December 21) while Mill (March 22) and Deer (March 29) creeks had the latest timing. Butte Creek, which dominated the aggregated abundance at Delta entry due to its higher outmigrant abundance combined with higher RST to Delta survival rates, had intermediate median arrival timing (February 15). The median arrival date in the Delta for the across-tributary aggregated stock was February 15, which was two to three weeks later than estimates of median arrival date at Tisdale (February 1) and Knights Landing (January 25) based on observed catch at these RST sites on the mainstem Sacramento River. Although we would expect passage timing to be later at Delta entry compared to the Tisdale and Knights Landing RST sites, which are 90 kilometers (km) and 61 km upstream of the Delta, we expect planned improvements to run type assignment from the PLAD models to narrow the gap between tributary outmigration based passage forecasts and passage estimates based on observations at mainstem RSTs.

srJPE requires forecasts of covariate conditions to improve the precision and accuracy of juvenile abundance and timing forecasts. To date, analyses have evaluated observed covariates based on their ability to explain the historical interannual variation in juvenile abundance, outmigration timing, and downstream survival rates. However, to make forecasts of juvenile abundance and timing, forecasts of covariate values are needed. A logical next step in srJPE development is to explore the ability to forecast covariate values. Alternatively, forecast scenarios can be made for potential future discrete conditions, such as whether the hydrological year type is dry or wet. The historical analysis of covariate effects will be useful for prioritizing covariates forecasting efforts.

Contents

1	Introduction	1
2	Methods	3
2.1	Integrated Juvenile Production Estimate Model Predicting Out-migrating Juvenile Abundance at Delta Entry	3
2.1.1	Estimation of Juvenile Abundance by Tributary	3
2.1.2	Survival Rate from RST to Delta Entry	6
2.1.3	Application of srJPE to Highlight its Behavior	8
2.2	Model Predicting Timing of When Outmigrating Juvenile Salmon Reach the Delta	9
3	Results.....	13
3.1	srJPE Predicting Out-migrating Juvenile Abundance at Delta Entry	13
3.2	Model Predicting Timing of When Out-migrating Juvenile Salmon Reach the Delta	16
4	Discussion	17
5	Challenges and Proposed Solutions for Modeling the Feather River Juvenile Production Estimate	22
5.1	Complicating Issues	22
5.2	Proposed Solutions	24
6	Recommended Process for Updating Integrated Model and Submodels.....	26
7	References.....	29

Tables

Table 1.	Uncertainty in Across-tributary Sum of Forecasts at Rotary Screw Traps and at Delta Entry.....	Tables-1
Table 2.	Pre-season Forecast of Median Dates When 50% of Outmigrants Pass Rotary Screw Trap and Arrived in Delta ...	Tables-2

Figures

Figure 1. Map Showing Rotary Screw Trap Locations Used for Modeling	Figures-1
Figure 2. Structure of Integrated srJPE Model.....	Figures-2
Figure 3. Stock-recruit Model Predicting Abundance at Deer Creek Rotary Screw Trap	Figures-3
Figure 4. Forecasts of Spring-run Juvenile Outmigration Timing	Figures-4
Figure 5. Predicted Weekly Abundance from Models at Upper Battle Creek Rotary Screw Trap in 2024	Figures-5
Figure 6. Predicted Survival Rate Estimated by Cormack-Jolly-Seber Submodel	Figures-6
Figure 7. Predicted Survival Rate from Release Point to Delta Entry	Figures-7
Figure 8. Outmigration Timing for Spring-run and Median Fork Length	Figures-8
Figure 9. Median and 80% Credible Intervals of Survival Rate	Figures-9
Figure 10. Structure of srJPE Predicting Timing of Spring-run Outmigrants.....	Figures-10
Figure 11. Forecast Travel Time as a Function of Monthly Peak Flows and Fork Length	Figures-11
Figure 12. Forecast Travel Time from Rotary Screw Traps to Delta	Figures-12
Figure 13. Forecast Survival Rate from Rotary Screw Traps to Delta Entry.....	Figures-13
Figure 14. Summary of Prior and Posterior Distributions	Figures-14
Figure 15. Comparison of Transformed Prior and Posterior Distributions from Integrated srJPE Model	Figures-15
Figure 16. Integrated srJPE Model Predictions of Spring-run Abundance at Rotary Screw Trap Sites.....	Figures-17
Figure 17. Pre-season Forecasts of Outmigration Timing at Rotary Screw Traps and at Delta Entry.....	Figures-18
Figure 18. Pre-season Forecasts of Aggregate Juvenile Outmigration at Delta Entry	Figures-19
Figure 19. Feather River Map Showing Study Locations	Figures-20

Acronyms and Abbreviations

Term	Definition
°C	degrees Celsius
BT-SPAS	Bayesian Temporally Stratified Population Analysis System
CJS	Cormack-Jolly-Seber
CV	coefficient of variation
Delta	Sacramento–San Joaquin River Delta
JPE	juvenile production estimate
LOOCV	leave-one-out cross validation
PLAD	probabilistic length-at-date
RST	rotary screw trap
spring-run	spring-run Chinook salmon

1 Introduction

We developed a model, srJPE, that integrates a set of submodels to forecast the annual abundance of juvenile spring-run Chinook salmon (*Oncorhynchus tshawytscha*) (spring-run) expected to outmigrate from the Sacramento River watershed into the Sacramento–San Joaquin River Delta (Delta). The intended purpose of srJPE and its constituent submodels are to inform new measures to minimize the impact on spring-run caused by operations of the California State Water Project and the federal Central Valley Project, although the models are also expected to contribute to improvement of existing spring-run life cycle models or development of a new spring-run life cycle model.

srJPE can be used to forecast juvenile abundance at rotary screw trap (RSTs) sites where outmigrating spring-run are monitored in tributaries of the Sacramento River and at Delta entry (Figure 1). The model integrates predictions from three submodels:

- **A stock-recruit model** that forecasts annual outmigration abundance at RSTs based on the abundance of spawners and physical covariates (flow, water temperature, or discrete variables) in the forecast year (described in Chapter 7).
- **An inseason model** that uses estimates of cumulative abundance from the start of juvenile migration through a forecast week in the forecast year, and an estimate of the cumulative proportion of the juvenile run that has passed the traps by that week in the forecast year, to forecast annual outmigration abundance (described in Chapter 8).
- **A Cormack-Jolly-Seber (CJS) survival model** that forecasts survival rate and travel time from RST locations to Delta entry (described in Chapter 9).

These submodels were fit to historical data to estimate posterior distributions of model parameters, which can then be used in srJPE to make forecasts.

The prediction of annual outmigration abundance from the stock-recruit submodel provides the earliest pre-season estimates of expected juvenile abundance at RSTs. In srJPE, these estimates are used to define a prior distribution for the prediction of outmigrant abundance based on fitting to inseason outmigration data and potentially environmental covariate data at any point in time after outmigration has begun. Predictions of outmigrant abundance at RSTs and the survival rate from RST locations to Delta entry are then used in srJPE to forecast juvenile abundance at Delta entry. To date, srJPE is based on data from six tributaries with spring-run populations (Battle, Clear, Mill, Deer, and Butte creeks, and the Yuba River) (Figure 1). Chapters 4 and 5 describe how tributary and mainstem outmigrant abundance was modeled from RST catch data and Chapter 6 describes how probabilistic length-at-date (PLAD) models were used to assign run identification to estimate spring-run specific outmigrant abundance. srJPE will eventually be applied

to data from Feather River when predictions of the proportion of spring-run juveniles from the Feather River PLAD model become available. The challenges and proposed solutions for modeling the Feather River component of the spring-run JPE are discussed in more detail at the end of this chapter.

We also developed an outmigration timing model to provide a pre-season forecast of when outmigrating juvenile spring-run are expected to arrive in the Delta. This model combines forecasts of outmigration timing at RST sites (Chapter 8) with forecasts of travel time from RST sites to Delta entry (Chapter 9). Predictions of the abundance and arrival timing of spring-run juveniles in the Delta can support development of potential measures to protect spring-run from operations of State and federal water projects, and support development of other potential conservation actions.

2 Methods

2.1 Integrated Juvenile Production Estimate Model Predicting Out-migrating Juvenile Abundance at Delta Entry

srJPE uses a Bayesian statistical framework and is coded in Stan software (Stan Development Team 2023); refer to Appendix A for source code. In the equations that follow, model terms in boldface Roman letters identify variables that are derived from submodels and treated as data in srJPE (but with uncertainty), Greek letters identify estimated parameters in srJPE, and Roman plain-face letters identify derived variables. Roman plain-face letters are variables that are calculated based on estimated parameters, data, and assumed constants. Figure 2 shows an overview of model structure.

2.1.1 Estimation of Juvenile Abundance by Tributary

The forecast of the log of annual juvenile outmigrant abundance, v , at an RST site in tributary i_{trib} is assumed to be a random variable arising from a prior normal distribution with means $\text{prSRmu}_{i_{trib}}$ and standard deviation $\text{prSRsd}_{i_{trib}}$,

Equation 1.

$$v_{i_{trib}} \sim \text{normal}(\text{prSRmu}_{i_{trib}}, \text{prSRsd}_{i_{trib}}).$$

The log of annual outmigrant abundance from each tributary is then transformed to predict annual abundance, $N_{i_{trib}}$,

Equation 2.

$$N_{i_{trib}} = \exp(v_{i_{trib}}).$$

The mean and standard deviation for the prior distribution of v for each tributary (Equation 1) were calculated based on forecasts of annual outmigrant abundance from the stock-recruit submodel with the best predictive accuracy for each tributary, as determined by a leave-one-out cross validation (LOOCV) analysis. The stock-recruit submodel uses spawner abundance and continuous (e.g., water temperature over spawning and incubation period) or discrete (e.g., water year type) covariate value in the forecast year to predict a posterior distribution of annual outmigrant abundance (Korman et al. 2025a). **prSRmu** and **prSRsd** were calculated from the mean and standard deviation of log-transformed posterior samples of the forecast, respectively. Figure 3 is an example of a stock-recruitment relationship used for defining a prior distribution for annual outmigrant abundance. The variance in the posterior distribution of forecasted annual outmigrant

abundance from the stock-recruit model includes effects of both parameter uncertainty and unexplained process error, with the latter dominating the total variance.

srJPE estimates annual juvenile outmigrant abundance in the forecast year by fitting to inseason abundance data. Annual outmigrant abundance estimates from the stock-recruit model are used as prior distributions for abundance estimates from the inseason model. The first step in the inseason calculations predicts cumulative abundance from the start of the run through a forecast week using,

Equation 3.

$$Nx_{itrib,iwk} = \log(N_{itrib} \cdot \text{inv_logit}(\theta_{itrib,iwk})).$$

where:

Nx is the predicted cumulative outmigrant abundance through forecast week iwk in log space, and

θ is the estimated logit-transformed cumulative proportion of the juvenile outmigrant abundance that has passed the trap by the end of the forecast week.

The inv_logit term indicates the transformation of the proportion from logit space which restricts proportions to a value between 0 and 1.

θ is assumed to be a random variable arising from a normal distribution with mean $\text{cp_mu}_{itrib,iwk}$ and standard deviation $\text{cp_sd}_{itrib,iwk}$ using,

Equation 4.

$$\theta_{itrib,iwk} \sim \text{normal}(\text{cp_mu}_{itrib,iwk}, \text{cp_sd}_{itrib,iwk}).$$

The mean and standard deviation were calculated from the inseason timing submodel, which predicts the outmigration timing in a forecast year based on fits to historical data on weekly cumulative juvenile outmigration abundance (Korman et al. 2025b). This model can include covariate effects on outmigration run timing. As for the stock-recruit submodel, an LOOCV analysis is used to identify the covariate model with the best predictive out-of-sample accuracy for each tributary. The inseason submodel forecasts cumulative outmigration proportions for each week of the outmigration period in a forecast year. cp_mu and cp_sd were set to the mean and standard deviation of logit-transformed samples from the posterior distribution for forecast week iwk . Figure 4 shows outmigration-timing forecasts from this submodel.

The posterior distribution of ν was estimated by comparing predicted and “observed” estimates of log-transformed cumulative outmigrant abundance through the forecast week using the data likelihood,

Equation 5.

$$\text{obsNx_mu}_{\text{itrib},\text{iwk}} \sim \text{normal}(\text{Nx}_{\text{itrib},\text{iwk}}, \text{obsNx_sd}_{\text{itrib},\text{iwk}}),$$

where:

obsNx_mu and **obsNx_sd** are the mean and standard deviation of the “observed” log of cumulative abundance through forecast week *iwk*.

To derive these estimates, BT-SPAS-X (Korman et al. 2025c) is applied to weekly catch data in the forecast year to estimate weekly abundance of juvenile outmigrant abundance at an RST site (all run types combined; refer to the top panel of Figure 5). Posterior distributions of weekly all-run type abundance estimates are multiplied by weekly posterior distributions of the proportion of spring-run (Figure 5, middle panel) as determined by PLAD (Chapter 6), to generate a posterior distribution of spring-run juvenile abundance estimates for each week (Figure 5, bottom panel). These values are summed from the first week of the outmigrant run through the forecast week, and then log-transformed. **obsNx_mu** and **obsNx_sd** are then calculated as the mean and standard deviation of log-transformed cumulative abundance values. While srJPE treats estimates of cumulative abundance as data, it recognizes the uncertainty in the estimates via **obsNx_sd**.

Equation 5 represents the data likelihood of srJPE. During model fitting, estimates of ν (Equation 1) and θ (Equation 4) are adjusted so that predicted Nx is close to **obsNx_mu**. However, the fitting will not result in a perfect match between these later two variables because:

- The model admits that **obsNx_mu** is uncertain
- ν is not a completely free parameter owing to the influence of its prior distribution from the stock-recruit model (Equation 1)
- There is a cost to the adjustment of θ (to predict Nx via Equation 3) owing to its prior distribution (Equation 4)

Ultimately, the predicted posterior distribution of ν in a forecast year depends on the amount of information in its prior distribution as determined by the stock-recruit submodel, the amount of information about cumulative abundance through the forecast week as determined by **obsNx_sd**, and the amount of information about the cumulative proportion of the outmigrant run that has passed the trap through that week as determined by the inseason timing submodel. As shown in Section 3, the importance of these information components in the estimation of ν will vary across RST sites, and the importance of the latter two will also vary across forecast weeks within RST sites.

To understand the influence of the prior distribution of v on the posterior distribution of the annual abundance estimate, we calculated an independent inseason estimate of annual abundance, $ind_N_{itrib,iwk}$, using,

Equation 6.

$$ind_N_{itrib,iwk} = \frac{\exp(normal(obsNx_mu_{itrib,iwk}, obsNx_sd_{itrib,iwk}))}{inv_logit(normal(cp_mu_{itrib,iwk}, cp_sd_{itrib,iwk}))}.$$

Note here the independent estimate of annual abundance is a derived variable and thus does not have a prior distribution. As a result, random samples from the distributions in the numerator and denominator of Equation 6 will have the identical distributions to their priors. The differences in the posterior distribution of ind_N (Equation 6) and N (Equations 1 and 2) would thus be driven by the influence of the prior distribution on N (v) as determined by the forecast from the stock-recruit submodel.

2.1.2 Survival Rate from RST to Delta Entry

Forecasts of juvenile outmigrant abundance at RSTs from the tributary component of srJPE (N_{itrib}) are multiplied by forecasts of survival rate from RSTs to Delta entry to predict juvenile abundance at Delta entry. We used a Bayesian Cormack-Jolly-Seber (CJS) submodel fit to detections of fall- and spring-run hatchery- and wild-origin smolts that were acoustically tagged, to forecast survival rates (Cordoleani and Korman 2025).

To date, the model with the highest predictive accuracy included effects of fish size at release and maximum flow during the period of outmigration. The model was fit to data from over 11,000 acoustically tagged smolts (wild- but mostly hatchery-origin) released over multiple years in Battle Creek (Coleman National Hatchery), at Red Bluff Diversion Dam, in Mill, Deer, and Butte creeks, and in the Feather River. Posterior distributions of model parameters predicting survival rates were used to forecast size-flow-survival relationships for migration to Delta entry from RST sites located in upper Sacramento River tributaries (Battle, Clear, Mill, and Deer creeks), and from RST sites in Butte Creek (and Feather/Yuba River) (Figures 6 and 7).

The model predicts increasing survival with fork length and maximum flow during the period of release. Forecasts of survival rate include unexplained error, which was estimated based on across-release group random effects. For the forecast, we assumed that peak flows during outmigration in the forecast year were equal to the averages during release periods for upper Sacramento, Butte Creek, and Feather River. When applying the model for an actual forecast, projected peak flows during outmigration will be used.

Variation in fish size over the duration of the outmigration run, and the proportion of the run outmigrating at different sizes, needs to be accounted for in the forecasts

of survival rate from RST to Delta entry. For example, early in the run only recently emerged fish are present, so the mean size of outmigrants will be small. As the outmigration season progresses, some fish that emerged early but did not outmigrate have grown, so the mean size of outmigrants increases. In addition, the proportion of the outmigrant run that passes the trap is not constant over the outmigration season. For example, RST-Delta entry survival rates for fish outmigrating during the peak of the run should have a bigger effect on the season-average survival rate compared to survival rates occurring at the tails of the run. Thus, variation in fish size by week, and variation in the proportion of run passing the trap each week needs to be accounted for in the calculation of an annual RST-Delta survival rate.

The PLAD submodel predicts the size distribution of spring-run juvenile outmigrants by week in each year the model is applied. We calculated the median fork length of spring-run outmigrants across available years for each week from the PLAD predictions (red lines in Figure 8). These values were used as input to the CJS-based size-survival functions (Figure 6) to provide posterior distributions of RST-Delta entry survival rate for each week. To account for variation in the total outmigrant run passing the trap each week, a composite posterior distribution of survival rates was created. We used the inseason model forecast of the proportion of the run passing an RST site to calculate the proportion of outmigrants passing the trap each week (black lines in Figure 8). We then calculated the ratio of each weekly proportion to the minimum proportion across weeks, and rounded this value to an integer (weekly_weight). We then took 500 samples from each weekly posterior sample of survival rates based on the median fork length for that week, and replicated it by weekly_weight. The posterior samples from this composite posterior distribution were logit-transformed and used to calculate a mean (**S_mu**) and standard deviation (**S_sd**) for srJPE (Figure 2).

In srJPE, logit-transformed values of survival rate from RST to Delta entry (ϕ_{itrib}) were generated using,

Equation 7.

$$\phi_{itrib} \sim \text{normal}(\mathbf{S_mu}_{itrib}, \mathbf{S_sd}_{itrib})$$

Posterior distributions of transformed RST to Delta entry survival rates showed small differences among most tributaries (Figure 9). Distributions for survival from Battle, Clear, Mill and Deer creek sites were based on the same size-flow-survival relationship (Figure 6); thus, differences in forecasted survival rates among these sites were caused by differences in outmigrant run timing and size-at-outmigration (Figure 8). For example, survival rates were slightly higher for outmigrants from Deer Creek owing to its later outmigration timing when fish are predicted to be larger compared to other upper Sacramento River tributaries. Higher survival rates for outmigrants from Butte Creek and especially from the Yuba River RST were largely driven by closer proximity to Delta entry relative to other RST sites.

With estimates of survival rates from RST sites to Delta entry, tributary-specific juvenile outmigrant abundance at Delta entry ($D_{itrib,iwk}$) is calculated from,

Equation 8.

$$D_{itrib,iwk} = N_{itrib,iwk} \cdot \text{inv_logit}(\phi_{itrib}).$$

These values are summed across **Ntribs** tributaries (Battle Creek, upper Clear Creek, Mill Creek, Deer Creek, Butte Creek, Yuba River, Ntribs=6) to derive a juvenile production estimate at Delta entry in a forecast week (D_{iwk}) using,

Equation 9.

$$D_{iwk} = \sum_{itrib=1}^{itrib=Ntribs} D_{itrib,iwk}.$$

Note that simulated RST to Delta entry survival rates depend solely on their prior distributions (Equation 7). Simulated survival rates only impact estimates of D, and we do not assume any prior information about D. Thus, the extent of uncertainty in survival rates, as determined by S_sd, translate directly to uncertainty in the JPE at Delta entry.

2.1.3 Application of srJPE to Highlight its Behavior

To demonstrate the behavior of srJPE we used historical data to calculate inputs for a theoretical forecast year. srJPE was applied to data from six tributaries (Battle, Clear, Mill, Deer, Butte creeks, and Yuba River), and will eventually include data from Feather River when estimates of spring-run outmigrant abundance are available. Analyses of stock-recruit, inseason, and downstream survival submodels are ongoing. Thus, the versions of these submodels used for this analysis may change in the near future, and likely over the long term as additional data are collected and analyzed. However, existing versions of the submodels are sufficient for the purpose of describing the behavior of srJPE.

We used the multi-year average of spawner abundance from each tributary for brood years included in the stock-recruit analysis as surrogates for spawner abundances in a future forecast year. These abundances were used as input to the stock-recruit model to calculate the priors on annual juvenile outmigrant abundance via Equation 1. Redd counts were used to index spawner abundance for Battle, Clear, and Mill creeks, holding counts were used for Deer Creek, and carcass surveys were used for Butte Creek and Yuba River. We used stock-recruit models with the best out-of-sample predictive accuracy (Korman et al. 2025a) based on analyses conducted to date, which were:

- si_mean_flow (Battle Creek)
- si_weekly_max_temp_median (upper Clear Creek)
- si_gdd_spawn (Mill Creek)

- si_above_13_temp_week (Deer Creek and Yuba River)
- si_min_flow (Butte Creek)

To simplify the analysis, we assumed covariate conditions for stock-recruit models and the migration survival model (peak flow during outmigration) in the forecast year were equal to the historical averages.

Forecast dates were set to model weeks that ended on December 28, February 1, March 1, and March 29. These were the weekly model dates closest to the forecast weeks identified by the modeling advisory team of January 1, February 1, March 1, and April 1. We used the historical multi-year average cumulative juvenile outmigrant abundance estimates on each of these forecast dates at each RST site to define **obsNx_mu** used in the data likelihood of srJPE (Equation 5). We used the multi-year average of the variance estimates of cumulative abundance for each forecast date at each RST site to calculate **obsNx_sd**. Statistics on the cumulative proportion of outmigrants passing each RST site by forecast week (Equation 4) were based on the null inseason model, which does not include a covariate effect on outmigration timing, as the covariate analysis for this submodel has been very limited to date (Korman et al. 2025b).

2.2 Model Predicting Timing of When Outmigrating Juvenile Salmon Reach the Delta

Weekly variation in the proportion of spring-run juvenile outmigrants reaching the Delta is predicted based on forecasts of outmigration timing at RST sites from the inseason submodel (refer to Figure 4 in Chapter 8) and forecasts of travel time and survival rates predicted from the CJS survival-travel time model (refer to Figures 7, 8, 12 and 13 in Chapter 9). The latter model uses an annual forecast of peak monthly flows to predict travel time from RST locations to Delta entry (Figure 11, top row). Travel time decreases with increases in peak flows based on data from acoustically tagged fish released in spring-run-producing tributaries of the upper Sacramento River (Battle, upper Clear, Mill, Deer creeks), but increases with peak flows for fish released in Butte and Feather River. The longer travel times from these lower tributaries at higher flows are likely the result of fish routing through sloughs and bypasses which are only accessible at higher flows. Interestingly, the positive relationship between peak flows and survival rate was very strong for Butte Creek and Feather River (Figure 7) in spite of increased travel time at higher flows in these systems. Travel time forecasts also depend on fish size at outmigration. These sizes vary by tributary and outmigration week as determined from the PLAD model. Because fork length of outmigrants increases over the season (Figure 8) and travel time declines with increases in fork length (Figure 11, bottom row), the model predicts travel time declines over the outmigration season (Figure 12). The integrated timing model shifts the non-cumulative proportion passing an RST each week forward in time based on the forecasted travel time for that week. As travel

time declines over the outmigration season, it is possible fish passing the RST on a later week arrive in the Delta in the same week as a fish that passed the RST at an earlier week. This dynamic can result in a slightly steeper Delta arrival timing relationship compared to timing at the RST.

Forecasts of weekly survival rates from the CJS model are also used to weight the weekly proportions of fish arriving at the Delta. Survival rates are predicted to increase with fish size (Figure 6). As the size of outmigrating juveniles increases over the outmigration period (Figure 8), survival rates will increase over the outmigration season (Figure 13). This dynamic could also result in a slightly steeper Delta arrival timing relationship compared to timing at the RST. Currently, the integrated timing model does not allow survival rate to vary across weeks due to factors other than fish size, such as peak flows. However, the model can be modified if weekly forecasts of peak flow are available.

The calculations used to compute arrival timing begin with forecasts of the posterior distributions of the non-cumulative proportions of juveniles departing from an RST site in tributary i_{trib} for each model week i_{wk} ($pD_{i_{trib},i_{wk}}$). The week of arrival for any RST departure week (arr_wk) is simply the sum of that week's index and the weekly travel time from the RST to the Delta for that week (TT),

Equation 10.

$$arr_wk_{i_{trib},i_{wk}} = i_{wk} + TT_{i_{trib},i_{wk}}.$$

Note that TT is a posterior distribution, thus this equation predicts a posterior distribution of arrival times. TT is predicted in units of days based on the forecasts from the CJS survival-travel time model, converted to units of weeks, and then rounded to the nearest week so it can be used to identify an array element. The non-cumulative probability of arrival for each week ($pA_{i_{trib},i_{wk}}$) can then be computed by summing up pD's across all weeks with the same arrival weeks using,

Equation 11.

$$pA_{i_{trib},arr_wk_{i_{trib},i_{wk}}} = \sum_{i_{wk}=1}^{i_{wk}=53} pD_{i_{trib},i_{wk}} \cdot \bar{\phi}_{i_{trib},i_{wk}}$$

As travel time can change across weeks it is possible than different RST departure weeks have the same arrival weeks. There can also be some weeks with no predicted arrivals. In Equation 11, note that each weekly RST departure probability is weighted by the forecasted mean survival rate from the RST to Delta for that week ($\bar{\phi}$). This accounts for differential survival rates over the duration of the run. Thus, RST departure probabilities for weeks with lower survival rates to the Delta would make less of a contribution to the Delta arrival timing relationship compared to weeks with higher survival. We used the mean survival rate for each week rather

than the posterior distribution of the weekly survival rate (as we did for travel time in Equation 10) because this led to unrealistic predictions of uncertainty in arrival timing owing to the very large uncertainty in weekly survival rates (Korman and Cordoleani 2025).

Cumulative timing relationships (cpD and cpA) are then computed using,

Equation 12.

$$cpD_{i\text{trib},i\text{wk}} = \frac{\sum pD_{i\text{trib},1:i\text{wk}}}{\sum pD_{i\text{trib},1:53}}$$

$$cpA_{i\text{trib},i\text{wk}} = \frac{\sum pA_{i\text{trib},1:i\text{wk}}}{\sum pA_{i\text{trib},1:53}}.$$

Finally, tributary-specific predictions of outmigrant RST departure timing and arrival timing in the Delta are combined to predict aggregate timing relationships. As there can be large differences in the abundance of outmigrating juveniles across tributaries, weekly values for the aggregate RST departure timing relationship are calculated by summing the product of the tributary-specific non-cumulative weekly departure proportions and tributary-specific forecasts of annual abundance ($W_{i\text{trib}}$) using,

Equation 13.

$$pD_{i\text{wk}} = \sum_{i\text{trib}=1}^{i\text{trib}=N\text{tribs}} pD_{i\text{trib},i\text{wk}} \cdot W_{i\text{trib}}$$

$$cpD_{i\text{wk}} = \frac{\sum pD_{1:i\text{wk}}}{\sum pD_{1:53}}.$$

For a pre-season forecast of aggregate timing, the weights for each tributary ($W_{i\text{trib}}$) are calculated using abundance forecasts from the stock-recruit models ($W_{i\text{trib}} = e^{prSRmu_{i\text{trib}}}$). Alternatively, an in-season forecast of the RST departure timing for the aggregate uses forecasts of tributary-specific outmigrant abundance from srJPE (Equation 2) for the weighting factor ($W_{i\text{trib}} = N_{i\text{trib}}$).

For the Delta arrival timing relationship, a pre-season estimate of aggregate weekly non-cumulative abundance (N_pA) is calculated by multiplying tributary-specific Delta arrival probabilities and the product of tributary-specific outmigration abundance and mean survival from RST to the Delta ($W_{i\text{trib}} = e^{prSRmu_{i\text{trib}}} \cdot \phi_{i\text{trib},i\text{wk}}$) using,

Equation 14.

$$N_pA_{i\text{wk}} = \sum_{i\text{trib}=1}^{i\text{trib}=N\text{tribs}} pA_{i\text{trib},i\text{wk}} \cdot W_{i\text{trib}}$$

$$cpA_{i\text{wk}} = \frac{\sum N_pA_{1:i\text{wk}}}{\sum N_pA_{1:53}}.$$

The weighting accounts for variation in both annual outmigration abundance across tributaries, and variation in RST-Delta survival rates across tributaries and model weeks. The aggregated arrival timing to the Delta can also be computed using an in-season forecast of tributary-specific outmigration abundance from srJPE ($W_{itrib} = N_{itrib} \cdot \bar{\phi}_{itrib,iwk}$).

3 Results

3.1 srJPE Predicting Out-migrating Juvenile Abundance at Delta Entry

To highlight the influence of forecast date and the use of a stock-recruit based prior for srJPE, we compared posterior distributions of annual juvenile outmigration at RST sites from srJPE to the independent inseason and stock-recruit models, noting that the stock-recruit-model predictions served as the prior distributions for srJPE (Figure 14).

The results from upper Clear Creek, compared to the other sites, were relatively precise for the earliest independent inseason prediction date (Equation 6). This was because outmigration run-timing is early in Clear Creek, so the majority of fish have outmigrated prior to the first forecast week (Figure 4), leading to high certainty in the proportion of outmigrants that have passed the trap even for the earliest forecast week. However, the unique early outmigration timing for the Clear Creek RST site (Figure 4) also meant that there was very limited increase in the precision of the Clear Creek outmigration abundance forecast from first to last forecast weeks from srJPE, because the amount of information about abundance from the inseason component of the model did not increase much after the initial forecast date. The stock-recruit-based prior on outmigrant abundance for upper Clear Creek was moderately precise (i.e., 80% credible interval ranges from approximately 25,000–150,000 fish), but had a lower median than the independent inseason estimates (Figure 14). This caused the median of srJPE predictions to be lower than those from the independent inseason model due to the constraining effect of the prior distribution from the stock-recruit model.

Compared to Clear Creek, results for the Mill Creek RST site and the other sites were more variable across forecast weeks and improved in certainty as the migration season progressed (Figure 14), due to later outmigration run-timing (Figure 4). The stock-recruit-based prior on Mill Creek outmigration abundance was relatively imprecise (i.e., 80% credible intervals of approximately 0 to greater than 200,000). However, the independent inseason estimate of abundance on the first forecast week (December 28) was even more uncertain (Figure 14) because only a small proportion of juveniles typically pass the RST site by this date. Across years, there was a reasonably high probability that the proportion was close to zero on the first forecast week (Figure 4), resulting in a very large upper credible interval for the independent inseason abundance estimate. In this situation, the stock-recruit based prior on annual outmigration abundance had a dominant influence on the posterior even though the prior was relatively imprecise. By the third forecast week (March 1), a higher proportion of outmigrants are estimated to have passed the RST site (Figure 4), resulting in a substantive increase in information about annual abundance from the inseason submodel, which in turn resulted in a higher median

and narrower credible intervals of the posterior (Figure 14). Because of the high uncertainty of the stock-recruit based prior (noted above), the posterior prediction of srJPE was nearly identical to the independent inseason-based prediction for all forecast dates.

Results for the Butte Creek RST site generally follow the same increase in independent inseason model predictions as seen for Mill Creek. However, unlike Mill Creek, there was substantial influence of the stock-recruit based prior on srJPE's prediction for the first forecast date due to high uncertainty in the independent inseason prediction. The influence of the prior on srJPE median prediction diminished for later forecast dates as the amount of information in abundance from inseason sources increased the precision of srJPE's forecast (Figure 14). In this example the median of independent inseason estimates of abundance were considerably higher than the median of the stock-recruit-based prior.

To further illustrate the inner workings of srJPE, we compared prior and posterior distributions of all random variables using results for upper Battle and Mill creek RST sites as examples. The good correspondence between prior and posterior distributions of annual outmigrant abundance for Battle Creek on the first forecast week (upper-left panel in Figure 15a) indicates one of two things: a) data driving the data likelihood are consistent with the stock-recruit-based prior distribution, or b) information sources are not consistent and the prior distribution is dominating the data likelihood. The consistency between the prior and random samples for the cumulative abundance on this forecast date (second row-left column of Figure 15a) indicates that cumulative abundance estimates though this forecast week are consistent with the priors (independent estimates from the numerator of Equation 6). However, the random samples of the proportion of outmigrants that have passed the RST had a higher mean than the prior (denominator of Equation 6, bottom row-left column of Figure 15a).

Given the considerably lower median outmigrant abundance of the stock-recruit-based prior compared to the independent inseason estimate on the first week (Figure 14), srJPE simulated a slightly higher cumulative proportion passing the RST by this forecast week (bars in bottom left panel Figure 15) than the independent estimate of this proportion (the prior, dashed line). In short, srJPE discounted the limited information on run-timing from the inseason model on the first forecast week because there was more information in the stock-recruit-based prior on annual abundance (which indicated lower abundance) and in the cumulative abundance through the forecast week. In this case, the best way for srJPE to maximize probabilities across the two priors (log abundance and logit cumulative proportion passing trip through forecast week) and the data likelihood (log of cumulative abundance through forecast week) was to increase the probability penalty for the logit cumulative proportion component of the model.

The prior distribution for annual outmigrant abundance for Mill Creek was much less informative than the one for Battle Creek (note flat distribution in transformed space) and thus had a negligible influence on posterior distributions (Figure 15b, top row). As a result, the posterior distributions for inseason estimates of outmigrant abundance and proportions passing the trap were very similar to the independent estimates (middle and bottom rows), because there was no conflict between the prior and posterior distributions of annual abundance.

Outmigrant abundance summed across RST sites was dominated by predictions from Butte Creek owing to its substantively higher juvenile production compared to other tributaries (Figure 14). We suspect the spring-run juvenile abundance estimates for the Yuba River site are biased high. Average spawner abundance based on carcass surveys in Butte Creek and Yuba River used in the stock-recruit analysis were similar (approximately 7,500 fish), yet juvenile abundance from Yuba River was 10-fold greater (Korman et al. 2025a). Estimated maximum egg-outmigrant survival rates in Butte Creek were realistic (19%) while those from Yuba River were not (381%). Results from the PLAD model for the Yuba River site require further examination as they may be overestimating spring-run proportions as occurred at the lower Clear Creek RST site (Korman et al. 2025c). In the case of Clear Creek, we concluded that small error rates in the PLAD causing assignment of genetic fall-run to spring-run were greatly magnified by a high relative abundance of fall-run compared to spring-run.

The sum of annual juvenile outmigration abundance estimates exiting tributaries at RST sites and surviving migration from tributaries to the point of Delta entry, without inclusion of estimates from Yuba River and Feather River, are provided in Figure 16. The median estimates of total abundance exiting tributaries based on the latest forecast date was 2.8 million fish with an 80% credible interval of 2.3–3.3 million fish. The median estimates of abundance at Delta entry based on the latest forecast date was 0.48 million fish with an 80% credible interval of 0.15–2.3 million fish. The ratio of median estimates of abundance at Delta entry to abundance at RST sites was 0.17. This ratio represents the RST abundance-weighted average of forecasted survival rates from tributary RSTs to Delta entry.

There was considerable uncertainty in forecasts of survival rate from tributary RST locations to Delta entry (Figure 9), leading to higher uncertainty in forecasted Delta entry abundance compared to abundance at RST locations (Figure 16). Relative uncertainty in the sum of abundance estimates across tributary RST sites, expressed as the coefficient of variation (CV) of posterior distributions, decreased from 1.02 to 0.11 between the first and last forecast weeks (Table 1b). This difference was driven by the substantively reduced uncertainty in inseason estimates of abundance for later forecast weeks, especially at the Butte Creek site, which dominated the total abundance estimate (Figure 14). The CVs of posterior distributions of abundance at Delta entry also declined for later forecast weeks, but not at the same rate as tributary RST sites (Table 1b). For example, on the last

survey date there was relatively little uncertainty about tributary production ($CV=0.11$) yet uncertainty in abundance at Delta entry was still moderately high ($CV=0.74$). This occurred because uncertainty in survival rates from RSTs to Delta entry becomes the main source of error in the JPE forecast as error in tributary outmigrant abundance declines.

3.2 Model Predicting Timing of When Out-migrating Juvenile Salmon Reach the Delta

Forecasts of the timing that outmigrant juveniles arrive at the Delta were very similar to the timing of when they passed RSTs (Figure 17; note almost complete overlap in 80% credible intervals). This occurred because travel time was relatively short (typically one to two weeks; Figure 12) in the context of the approximately 30 weeks in a year when outmigration can occur. The date when 50% of spring-run outmigrants arrived in the Delta varied considerably across tributaries. Clear Creek had the earliest timing (December 21) while Mill (March 22) and Deer (April 5) creeks had the latest timing (Table 2). Butte Creek, which dominated the aggregated abundance at Delta entry due to its higher outmigrant abundance (Figure 14) combined with higher RST to Delta survival rates (Figure 9), had intermediate arrival timing (February 15).

To provide an out-of-sample test of predictions of timing at Delta entry from the integrated timing model, we compared the tributary aggregate arrival timing to the Delta with estimated arrival timing based on observed catch at Tisdale and Knights Landing RST sites on the mainstem Sacramento River (Figure 18). The aggregated tributary estimate was based on forecasts from the inseason timing models for Clear, Battle, Mill, and Deer creeks (Figure 4), tributaries that enter the mainstem above the Tisdale and Knights Landing mainstem RST sites (Figure 1). The median estimated arrival date in the Delta for the across-tributary aggregated stock (Clear, Battle, Mill, and Deer creeks) was March 29, which was approximately two months later than estimates of median arrival date at Tisdale (January 25) and Knights Landing (February 1) RST sites based on observed catch (Figure 18).

4 Discussion

srJPE provides a robust approach to forecast spring-run juvenile abundance and timing at Delta entry by combining information from submodels predicting juvenile outmigrant abundance at RST sites (stock-recruit, inseason), and from the CJS submodel predicting survival rates and travel time from RSTs to Delta entry. One key advantage of srJPE is that it does not require a user to decide when to switch from pre-season stock-recruit to inseason approaches to forecast abundance at RST sites. Such decisions would be difficult because the amount of information about annual abundance at RST sites from these two sources varies across tributaries for both models, and across forecast weeks within tributaries for the inseason model. srJPE provides a repeatable approach for blending information and will produce more precise JPEs because it maximizes the use of all available information on the date a forecast is needed.

This chapter demonstrates how srJPE works, and is not intended to provide definitive JPE forecasts at this time. Estimates of juvenile outmigration abundance and timing at RST sites and Delta entry presented here should be considered preliminary for a number of reasons. Currently, JPE forecasts in this chapter do not include estimates of natural- and hatchery-origin juvenile abundance from the Feather River. Modifications to the PLAD model (Chapter 6) are currently underway to account for the complexities of run type structure in the Feather River system owing to hatchery production and other factors (as discussed in more detail here in Section 5). We expect JPE forecasts to increase substantially when Feather River estimates are included in the model. Additional work on PLAD predictions at the Yuba River RST site are also required before Yuba River juvenile production is included in the JPE. In addition, all the submodels used in srJPE should be considered a work in progress. We anticipate that predictions will change as new data are added, and they may change substantively if new covariates are evaluated. This is undoubtedly true for the inseason model where only one covariate effect on one component of outmigration timing (median run date) has been explored to date (Korman et al. 2025b). Uncertainty in estimates of survival rate from tributary RST sites to Delta entry are a significant component of the total uncertainty in JPE forecasts from srJPE, especially later in the outmigration season when precision of abundance forecasts at tributary RST sites is higher. We recommend continued exploration of new covariates for the CJS survival model.

Our predicted timing of Delta entry using srJPE extended substantially longer into the migration season than estimates of arrival timing based on catch at the mainstem Tisdale and Knights Landing RST sites (Figure 18). There are a number of reasons why the srJPE prediction of arrival timing could differ from the estimates based on observed catch. We first address possibilities that we consider less likely to explain the discrepancy, and then discuss explanations we consider to be more plausible.

Our travel time predictions were from tributaries to Delta entry rather than to the Tisdale and Knights Landing RST sites, and the location of Delta entry is 96 km downstream from the Tisdale RST site and 47 km downstream from the Knights Landing RST site. However, the effect of this longer distance on the difference in arrival timing between the RSTs and Delta entry would be a very minor component of the discrepancy. srJPE predicts an average travel time in the Butte-Sacramento reach of 1.7 days per 100 km. Thus, the additional time to travel between mainstem RST sites to the Delta entry point would be up to two days at most, which is much less time than the approximate two-month discrepancy. It is also very unlikely that error in srJPE prediction of a two-day travel time between the mainstem RSTs and Delta entry explains the discrepancy. The size of outmigrants leaving RST sites is much smaller than the range of sizes for telemetered fish used to fit the travel time model (Figure 11b). Thus, it is possible (and more likely) that travel time for smaller fish is actually longer than predicted by the travel time model.

Accounting for this longer travel time would cause the srJPE-predicted passage to be even later than reflected in Figure 18, and result in an even greater discrepancy with estimated passage based on observed catch at the mainstem RST sites. Another possible cause of the discrepancy is that the survival model is over-predicting migration survival later in the migration season. If this were the case, as the season progressed, fewer and fewer outmigrants would pass the mainstem RSTs compared to the srJPE prediction. This would require the survival model to become less accurate for fish outmigrating later in the migration season, which is unlikely because these later outmigrants would be larger fish and closer in size to the fish used for the acoustic telemetry survival studies.

A more plausible explanation for the discrepancy between the srJPE prediction and RST catch-based estimates of arrival timing is related to uncertainty and biases in the estimates based on catch observations at mainstem sites. Mainstem RST efficiencies and efficiency estimates are very low (as described in Chapter 5), resulting in generally high uncertainty in the estimated passage timing of juvenile salmon at mainstem RST sites. If catch efficiency declined systematically later in the migration season, this would make efficiency estimates less certain and more potentially biased high, which would cause passage estimates based on observed catch to be biased low later in the season, and cumulative passage estimates to be biased earlier. A systematic decline in efficiency could occur later in the season if later-migrating juveniles more successfully avoid capture in the RSTs due to their larger size or due to systematically changing conditions that influence catch efficiency, such as generally lower turbidity later in the migration season. Other speculative causes of lower efficiency could be examined, such as whether managed spring flow pulses from reservoirs later in the season are accompanied by smaller increases in turbidity compared to runoff pulses from natural storm events.

Another plausible explanation for the discrepancy shown in Figure 18 is that PLAD model increasingly underestimate spring-run proportions at the mainstem RST sites as the migration season progresses, or conversely the PLAD model increasingly overestimates spring-run proportions at the tributary RST sites as the season progresses. Increasing underestimates at the mainstem RST sites could occur because aggregated populations from multiple tributaries with different emergence timing and growth rates are passing the mainstem RSTs, resulting in increasing overlap in fork lengths across run types. Misassignment of later migrating spring-run as fall-run could cause considerable bias in PLAD estimated spring-run proportions at mainstem RST sites and could explain why passage estimates based on observations of mainstem catch ends earlier than passage based on outmigration observed in tributaries.

If spring-run at mainstem RSTs are increasingly assigned by PLAD to fall-run as the season progresses, outmigration patterns from Mill Creek and especially Deer Creek could be the culprit. Mill and Deer creek spring-run rear in colder water, grow more slowly, and outmigrate later in the season than spring-run in other tributaries (Figure 8). This delayed outmigration results in Mill Creek and Deer Creek spring-run being larger at outmigration compared to outmigrants from other spring-run populations in the Sacramento Valley (Figure 8), but the slower growth of Mill Creek and Deer Creek spring-run makes them smaller at any given date relative to fall-run outmigrants compared to relative sizes of spring-run and fall-run in other spring-run tributaries. This occurs because Mill Creek and Deer Creek fall-run grow and rear in warmer waters on the valley floor, and grow more quickly than the spring-run rearing at higher elevations. PLAD models specific to Deer Creek and Mill Creek are better able to account for these tributary specific patterns in spring-run and fall-run size-at-date compared to mainstem PLAD models. Since outmigrants from Deer Creek dominate the spring-run abundance at Tisdale and Knights Landing RST sites (Figure 17), this could result in late-migrating Deer Creek spring-run being misassigned to fall-run at the mainstem site, causing the severe truncation of the estimated spring-run passage timing based on mainstem RST catch seen in Figure 18.

To increase confidence in JPE forecasts, predictions from srJPE and its submodels should be tested using out-of-sample data. These tests may reveal model limitations and identify ways to improve predictions. The comparison of aggregate arrival timing in the Delta against independent forecasts of timing at Sacramento River mainstem sites (Tisdale, Knights Landing) provided in this chapter are a good example of the utility of such out-of-sample testing. A similar effort might compare predictions of juvenile abundance at Delta entry from srJPE with abundance estimates at the Tisdale and Knights Landing RST sites. The BT-SPAS-X and PLAD models could be applied to data from the Red Bluff Diversion Dam RST site to estimate spring-run juvenile abundance and timing to compare with the sum of juvenile abundance estimates and timing from Clear and Battle creeks predicted by the stock-recruit and inseason submodels. Predictions of juvenile spring-run

abundance can also be compared between RST sites in tributaries with more than one RST site. For example, we found that estimates of spring-run juvenile abundance at the lower Clear Creek RST site were 15-fold higher than at the upper site, which was unrealistic given limited spring-run spawning between trapping sites (Korman et al. 2025c). In addition, the productivity (outmigrants/spawner) at the lower Clear Creek site from the stock-recruit analysis was unrealistically high. Together these data supported the conclusion that PLAD-based predictions of spring-run proportions in RST catches at the lower site were too high due to misclassification of fall-run fish. Similar efforts could be conducted using multiple trapping sites in Battle Creek and Feather River to identify potential sources of bias.

srJPE requires forecasts of covariate conditions to improve the precision and accuracy of juvenile abundance forecasts. To date, historical data on covariate values have been used to identify the most predictive submodels to use for forecasting. These analyses define the covariates that best explain the historical interannual variation in juvenile abundance, outmigration timing, and downstream survival rates. However, to make a forecast of juvenile abundance, covariate values in the forecast year are needed. A logical next step in JPE model development is to explore the ability to forecast covariate values. In many cases it will not be possible to forecast a continuous covariate (e.g., maximum flow in the mainstem Sacramento during outmigration, or water temperature in a tributary); however, it may be possible to forecast discrete covariate levels (e.g., low-, intermediate-, and warm-temperature classes). The effects of forecasted covariate values on uncertainty in model predictions can be evaluated by applying covariate forecasting methods to historical data. Model predictions of juvenile abundance, outmigration timing, or downstream survival rates based on a forecasted discrete or continuous covariates could then be compared to the prediction from the historical covariate data. If forecasting covariates is not possible, srJPE can still be run under different assumed covariate conditions to produce forecast scenarios (e.g., low, moderate, and high flows during outmigration). Managers could then use the different JPE forecast scenarios to make decisions. In addition, the JPE model could be run using null submodels, which do not require covariate inputs. This is the simplest alternative but will result in higher uncertainty in JPE forecasts. We recommend that hydrologists, operation engineers, and the srJPE modeling team work together to identify the most appropriate methods to forecast covariate values for application in JPE forecast models. The historical analysis of covariate effects summarized in submodel reports will serve as useful guide to determine which covariates to focus on initially.

The current version of the integrated Delta arrival timing model does not account for weekly variation in survival rates or travel times over the outmigration season due to environmental factors like flow. The initial version of the model described here uses an annual forecast of peak flows over the entire migration period. This was done because we assumed that forecasting weekly peak flows would be very difficult and highly uncertain. However, analysis of historical data could be used to

estimate a distribution of peak flows by model week in say critically dry, below- and above-normal, and wet water year types. These distributions could then be used to simulate weekly peak flow values to adjust weekly survival and travel time values in the calculation of the arrival timing relationships. If higher peak flows are more likely in say, January and February in wetter years, this more-complex model would result in a higher proportion of arrivals earlier in the outmigration season due to both higher survival rates and shorter travel times under these conditions.

Decisions on how to develop and use JPE abundance and timing forecasts should be driven by management needs, and the way we summarized results in this chapter is not intended to be a final approach. For example, we selected 80% credible intervals to quantify uncertainty to highlight key dynamics of the model. This narrower interval made it easier to examine differences in prior and posterior distributions across survey dates and tributaries. A wider credible interval (e.g., 95%) may be preferred by some decision-makers when using srJPE to minimize take or evaluate other conservation measures. We also used a wide range of forecast dates in this chapter to demonstrate the tradeoff between the date a forecast is generated and the precision of an abundance estimate. Results logically show that earlier forecast dates, while more timely for some management decisions, have substantively higher uncertainty in forecasts compared to those made on later dates when juvenile outmigrant abundance is better defined by the inseason model. srJPE is set up to forecast JPEs for any dates they may be needed, and earlier dates may be weighed against the tradeoff of reduced precision to determine the best date given the objectives of a management action. Finally, during an earlier review of srJPE, some decision-makers expressed the desire to forecast JPEs using only the stock-recruit or inseason models to predict outmigrant abundance at RST sites. This user-defined approach is logical if there is concern that the one of these submodels provides a biased or unrealistic set of predictions. srJPE is easily modified to accommodate a user-defined selection of submodels to use for the forecast. If JPE forecasts based on stock-recruit priors combined with fitting to inseason estimates are used in decision-making, we recommend continuing to compare independent and integrated estimates of abundance at RST sites so that the contributions from the two information sources are well understood.

In this chapter, srJPE includes computation of a pre-season estimate of Delta arrival timing of populations from different spring-run tributaries, and for the aggregate population. In mixed-stock salmon fisheries, populations of different productivities or abundances are exposed to the same fisheries, and this information on tributary-specific outmigration timing could be used to tailor protections for more sensitive stocks.

5 Challenges and Proposed Solutions for Modeling the Feather River Juvenile Production Estimate

Modeling Feather River salmon is complicated by several issues. To understand these issues and propose potential solutions, it is first helpful to understand the hydrological and geomorphological characteristics of the Feather River and how it interacts with hatchery practices, environmental conditions, relationships with and between hatchery and natural-origin spring- and fall-run populations, and monitoring to track these dynamics.

5.1 Complicating Issues

Hydrological and geomorphological characteristics. Most of the historical habitat for Chinook salmon on the Feather River is blocked by Oroville Dam. To provide mitigation for this impact, the Feather River Hatchery is located just downstream from Oroville Dam on the Feather River (Figure 19). Downstream from the hatchery, a diversion shunts part of the below-dam flow into Thermalito Forebay and Afterbay, which is a complex designed for power generation and as a water-warming basin for agricultural use. Some of the water diverted into Thermalito Afterbay is returned to the Feather River further downstream. The reach between the diversion and the return is called the “low flow channel,” and the river below the return is called the “high flow channel.”

Cross-breeding of spring-run and fall-run. The Feather River Fish Hatchery produces both spring- and fall-run Chinook salmon, and salmon also spawn in-river upstream of the high flow channel. Spring-run have also spawned downstream of the high flow channel, but this has been rare in recent years. Although spring-run and fall-run enter the Feather River many months apart, their spawning periods overlap. This is because spring-run adults enter the system with immature eggs and oversummer in coldwater pools until eggs mature and spawning commences in the late summer, which is the same time of the year when fall-run adults migrate from the ocean and begin spawning with already matured eggs. Prior to the building of Oroville Dam, spring- and fall-run spawners were spatially segregated because higher flows during the spring allowed spring-run to access higher elevation parts of the river system where springs and snow melt maintained coldwater pools, and spring-run adults could oversummer. Since the building of Oroville Dam, spring-run are holding oversummer and spawning in the remaining coldwater reaches below the dam, a reach that is easily accessible to fall-run, which leads to a spatial overlap of spring- and fall-run adult spawning. This resulted in fall-run and spring-run historical crossbreeding in the hatchery and among natural spawners in the river, and to the production of offspring that were heterozygous for genetic markers associated with early versus late run-timing. To minimize spring-

and fall-run crossbreeding, the hatchery began tagging spring-run adults that cycled through the hatchery during the spring-run migration season, and then only used these tagged salmon as spring-run broodstock when they re-entered the hatchery during spawning season. However, not all spring-run enter the hatchery and get tagged each year, which continues to result in some crossbreeding of untagged spring-run selected for fall-run broodstock. In addition, crossbreeding undoubtedly continues among natural spawners given the lack of spatial segregation. This results in a significant portion of heterozygous run-timing genotypes among Feather River juveniles.

Run assignment policy and modeling issues. Currently, the policy for outmigrant run assignment is to use run-timing specific genetic markers to assign fish homozygous for early-running genotype to spring-run and those homozygote for late-running genotype to fall-run. Juveniles heterozygous for the run-timing markers are assigned to either spring- or fall-run using a suite of other genetic markers, which are not associated with run-timing but are based on similarities or differences in genetic composition with the spring-run population or fall-run population. These heterozygous early/late juveniles may outmigrate across a range of sizes and dates such that heterozygous juveniles assigned to spring-run by the population-based assignment method may outmigrate at a size and date closer to what is observed for fall-run and vice versa. This poses a problem for fitting PLAD models, which are trained on more recent years of data with genetic outmigrant assignments, and then used to assign run-type to years of catch data from before regular genetic testing. Given that most years of data currently available pre-date genetic testing, bias in PLAD-based assignments could lead to substantial bias in spring-run outmigrant abundance and timing estimates for these years, which then propagates through all Feather River-specific models. And given Feather River is annually either the largest or second-largest producer of naturally spawned spring-run in the Sacramento River watershed, this bias could have a substantial influence on the accuracy of the valley-wide spring-run JPE.

Other run assignment complications. Genetic testing in the Feather River is done on samples collected at the Eye Riffle RST site, which is situated at the downstream end of the low flow channel. However, most years of outmigrant catch data that overlaps with years of spawner abundance data are from the Herring Riffle RST site, which is 23 river kilometers downstream of the Eye Riffle RST site. Also, all spring-run spawning occurs upstream of Eye Riffle, while some fall-run spawned in the high flow channel (between Eye Riffle and Herring Riffle) in earlier years of the historical record, and juvenile production in this reach would not be accounted for in the Eye Riffle-based PLAD models. If this spawning produced a substantial number of fall-run, this could cause a temporally trending bias in the stock-recruit relationship. The original decision was that the additional information provided by more years of data from Herring Riffle outweighed the potential bias of using a PLAD model fit to length-at-date catch data at a site further upstream. However, initial stock-recruit relationships using Herring Riffle spring-run abundance

estimates produced unrealistically high production estimates for the number of spawners.

Finally, only 25% of each Feather River fall-run hatchery release are marked for identification, and occasionally only 50% of spring-run releases are marked (although 100% marking of spring-run is most common). In addition, over the past several years, the hatchery has released large numbers of unmarked fry-sized fall-run into the river that can only be identified by genetic testing. These unmarked hatchery fish migrate past some of the Feather River RST sites and may have different size and timing phenologies relative to natural production. This contribution of unmarked hatchery fish could interfere with the ability of PLAD models to predict run type of catch for years prior to genetic testing. The presence of unmarked hatchery fish in catch also requires many more genetic samples to be taken to identify naturally produced spring-run.

Ceratanova shasta parasite. *Ceratanova shasta* (*C. shasta*) is an endemic parasite that uses adult and juvenile salmon as an intermediate host, the other host being a polychaete worm. The greatest infection rates in the Central Valley are thought to occur in the Feather River, potentially accounting for a majority of juvenile mortality in some years. Water testing for the infectious spores that infect salmon indicates the most infectious zone begins where the Thermalito return flow enters the upstream end of the high flow channel, which is just downstream of the Eye Riffle RST site. This means stock-recruit models using Eye Riffle catch may not detect the influence of environmental conditions on *C. shasta* infection rates and disease outcomes (i.e., survival or death), such as water flow or temperature, which may cause an over-estimation of juvenile outmigrant abundance estimates from the Feather River.

Limited adult data. A major limitation to modeling stock-recruit relationships is the lack of naturally spawning spring-run adult abundance estimates prior to 2014 to match with RST data from 1998–2013.

5.2 Proposed Solutions

Model heterozygotes explicitly. To account for juvenile salmon with early/late run-timing genotypes (heterozygotes), we will model heterozygotes explicitly in PLAD models. The expectation is that heterozygous fish will exhibit intermediate outmigration length-at-date characteristics relative to fish with homozygous early and late genotypes. This may allow estimation of the proportion of heterozygous fish in RST data collected prior to regular genetic testing, which may help improve the accuracy of PLAD models. This will still require some means for assigning heterozygous fish in historical catch data to either spring-run or fall-run.

Use Eye Riffle RST data instead of Herring Riffle. We will switch BT-SPAS-X modeling from Herring to Eye Riffle to match the location of genetic testing and use this site for historical abundance modeling. We will combine Steep Riffle and Gateway Riffle data with the Eye Riffle data to increase the number of years in the Eye Riffle data set. All of these sites are in the low flow channel downstream of spring-run spawning locations, and the sites are close enough together to expect the PLAD model based on genetic sampling at Eye Riffle to apply at all three sites. Efficiencies will be modeled separately for each of these trapping sites.

Other potential solutions. Given there are multiple RST sites along the Feather River, we are considering modeling changes in abundance between these serially linked sites, potentially using a life cycle model framework, to better understand rearing mortality relationships to environmental conditions in the high flow channel (e.g., from pathogen infection or predation). This would provide alternative survival estimates to those based on acoustic telemetry using smolt-sized fish, and could be more applicable to pre-smolt outmigrants.

Accounting for hatchery production. We will model the hatchery production component of the spring-run population based on release number and estimated rearing and migratory survival rate. Because we will use the Eye Riffle to predict abundance of in-river production, we will not need to account for hatchery production because hatchery releases do not occur upstream of the Eye Riffle. For future modeling applications using RST data from lower in the system downstream of hatchery release locations (e.g., for alternative survival estimates described above), we will filter out the hatchery fish component of catch data based on PLAD distributions of marked juveniles in the RST catch data, which can be extrapolated to account for the unmarked component of hatchery release groups. The filtered catch data can then be used to estimate PLAD parameters for application to the natural production component at these RST sites. More recent completely unmarked fry releases will likely be accounted for using parental-based tagging, which identifies hatchery fish by genetic association with the genetic library of hatchery broodstock. PLAD models may be useful for targeting juvenile size ranges with the greatest uncertainty for genetic sampling and thereby reducing overall sampling needs to assess natural production.

Explore an alternative method for estimating adult abundance. We will investigate whether we can estimate naturally spawning adult spring-run abundance for additional years when spring-run adults were not specifically censused by comparing pre- and post-spawn adult tag rates among returning adults, although this would not account for spring-run that failed to enter the hatchery. This solution would be possible for the years after adult spring-run tagging was implemented in 2004.

6 Recommended Process for Updating Integrated Model and Submodels

We recommend three temporal scales for updating the submodels comprising srJPE, as outlined below. Additionally, we outline a process for updating models and establishing approval for model updates. The process for updating datasets to support model updates is described in Chapter 2.

Within-season updates. At the beginning of each migration season, the stock-recruit models should be run using up-to-date covariate data, including adult and redd survey data. During each outmigration season, the BT-SPAS-X and PLAD models could be run multiple times to provide up-to-date weekly all-run and spring-run juvenile outmigrant abundance estimates. This action could be done as often as weekly, or at specific dates during the outmigration season as needed, but would require RST catch and genetic datasets to also be updated for each model run. There would be no need to rerun BT-SPAS-X and PLAD for earlier years on a routine basis except when PLAD parameters are updated with new information, or after additional RST efficiency data are generated.

For the PLAD model, within-season updates could be made but would require genetic identifications to be completed on relatively short time frames (e.g., less than two weeks), which is feasible given current capabilities. Then the PLAD model coefficients would be modified through Bayesian updating using updated within-season catch and genetic datasets. This type of information could potentially come from specific high-sensitivity enzymatic reporter unlocking (SHERLOCK) assays (on the order of hours) or rapid turnaround of genetic samples using more traditional approaches (on the order of weeks).

Annual end-of-season updates. At the end of each outmigration season, after catch, efficiency, genetics, and covariate datasets have been checked for quality as part of the annual quality assurance and control process, all models should be refit to estimate fixed effect coefficients and random effects.

Multi-annual updates. Any changes in assumptions used in BT-SPAS-X (e.g., prior on upper limit of weekly abundances) or PLAD would require rerunning the models for all historical years. This would also be the case for the stock-recruit, in-season timing, and mainstem survival models. Note that new historical estimates of spring-run outmigrant abundance estimates due to changes in BT-SPAS-X or PLAD would require rerunning stock-recruit and in-season models since they depend on annual or weekly spring-run outmigrant estimates.

After several years of data collection, the PLAD model could re-evaluate the role of covariates in explaining annual variation in the model coefficients. Furthermore, this provides the opportunity to evaluate multiple model structures. The models can be

created by using annual covariates (e.g., temperature, relative spawning abundance, etc.), and linking them to coefficients via link functions (like a generalized linear model [GLM]). Model structures can also include alternative model functional forms, such as linear, polynomial, or thin-plate splines. The multiple model structures can then be evaluated to determine whether a single model or a weighted average of models provides the best predictive performance.

For PLAD, stock-recruit, in-season, and mainstem survival models, use of new covariates would require LOOCV testing of the new models and comparing performance to existing ones. If out-of-sample error of new covariates is lower, this new covariate would be used after discussion with review team. New covariates may include different discrete classifications, alternate ways of using the same continuous data (e.g., a different way of calculating temperature-dependent stress), or use of a new type of data. As more years of data are added, the models can accommodate more covariates.

Structural changes to any of the models would require rerunning all historical years. For example, predicting in-season run-timing based on covariate effects on run steepness, rather than median run date (current approach), would require evaluating this model relative to other models (based on LOOCV). If the new model outperforms historical models, the new structure would be used to calculate all historical years.

Any change to stock-recruit, in-season, timing, or mainstem survival models would require rerunning srJPE for all historical years.

Documentation and approval process. After model coefficients have been updated either within-season or annually with new data, these model fits need to be reviewed by the designated lead for the particular model. Leads should regularly inspect model fits for at least the first several years after a model's structure has been changed (including after srJPE is initially implemented). Over time the coefficient update process could become automated and require less frequent inspection. After the updated model fits are approved, model documentation and any automation scripts would be updated and the new model fit would be recorded as approved in the data store to keep track of model fit versioning and status.

Similar to the model fit review step, regular model output should be reviewed by the lead modeler or other designated reviewer with sufficient knowledge of the model and data. Over time, this step may become more automated as the models and workflow are improved and stable. For the models requiring weekly updates, this review interval could be relaxed depending on performance of the automated model output.

Updates of model covariates or structure require more thorough review. Similar to the review of initially implemented models, model updates should be reviewed and approved by a panel of interagency modeling experts and by regional monitoring staff with knowledge of the systems and populations being modeled. Updated model documentation should list the status and date of approval.

7 References

Stan Development Team. 2024. *Stan Users Guide*. Version 2.35. <https://mc-stan.org>

Tables and Figures

Tables

Table 1. Uncertainty in Across-tributary Sum of Forecasts at Rotary Screw Traps and at Delta Entry

Uncertainty in the across-tributary sum of forecasts of spring-run Chinook salmon (*Oncorhynchus tshawytscha*) (spring-run) juvenile abundance at rotary screw trap (RST) sites and at Delta entry. Statistics show the coefficient of variation (CV) of posterior distributions of abundance forecasts. Results are shown based on the sum of predictions from all tributaries that have been modeled (Table 1a) and all tributaries except Yuba River (Table 1b).

Table 1a. All Tributaries Modeled (Battle, Clear, Mill, Deer, Butte, and Yuba)

Forecast Week	CV at RST	CV at Delta
December 28	3.77 ^a	4.0 ^a
February 1	8.05 ^a	7.14 ^a
March 1	0.91	1.27
March 29	0.09	0.50

^a CVs for the first forecast week are not a reliable measure of uncertainty due to the very long right-hand tail of the posterior distribution (refer to Figure 12).

Table 1b. All Tributaries Except for Yuba (Battle, Clear, Mill, Deer, and Butte Only)

Forecast Week	CV at RST	CV at Delta
December 28	1.02	1.54
February 1	0.79	1.42
March 1	0.29	0.86
March 29	0.11	0.74

Table 2. Pre-season Forecast of Median Dates When 50% of Outmigrants Pass Rotary Screw Trap and Arrived in Delta

Pre-season forecast of the median dates when 50% of spring-run juvenile outmigrants have RST sites and arrived in the Sacramento-San Joaquin River Delta (Delta). Dates represent the end of each seven-day model week. Forecasts are provided for five tributaries and the aggregate relationship based on the weighted sum of tributary-specific timing. For comparison with the aggregate prediction, median outmigration dates at Tisdale and Knights Landing RST sites on the mainstem Sacramento River are also shown.

RST Site	RST	Delta
Battle Creek	January 25	February 1
Upper Clear Creek	December 7	December 21
Mill Creek	March 15	March 22
Deer Creek	March 15	April 5
Butte Creek	February 8	February 8
Aggregate	February 15	February 15
Tisdale	February 15	
Knights Landing	January 25	

Figures

Figure 1. Map Showing Rotary Screw Trap Locations Used for Modeling

Map of Sacramento River and tributaries showing the location of RSTs used in spring-run juvenile production modeling.

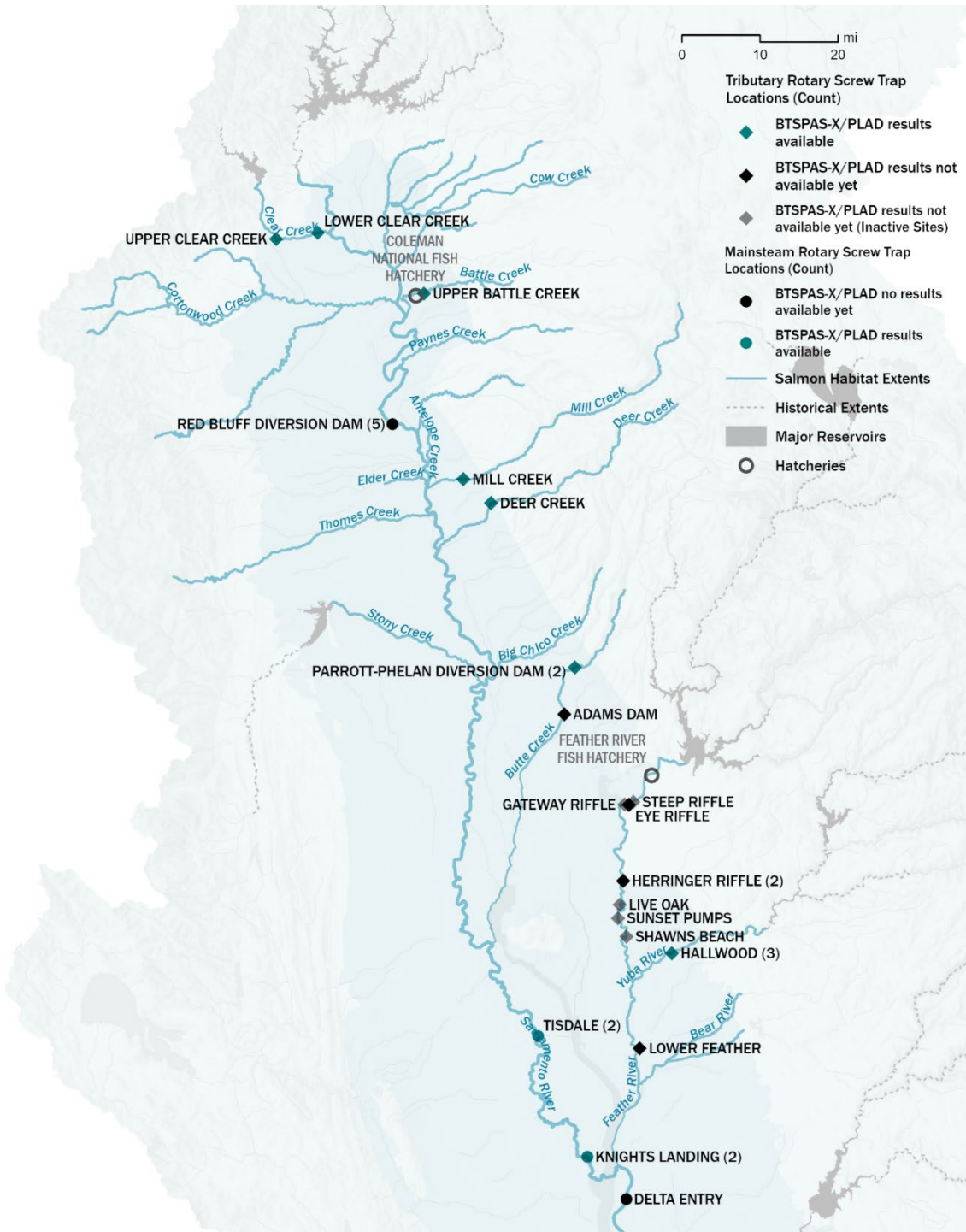


Figure 2. Structure of Integrated srJPE Model

Structure of integrated spring-run Chinook salmon Juvenile Production Estimate (srJPE) model, showing data inputs (bold text), key outputs (blue text), supporting submodels (*italics*), and inputs to submodels in a forecast year (red text). Posterior distributions of annual outmigrant abundance at RST sites and Delta entry (JPE) are estimated for each spring-run tributary with data, as denoted by the six tabs in the graphic (Battle, Clear, Mill, Deer, Butte creeks, Yuba River, and Feather River in the near future). These posteriors are summed across tributaries to derive system-wide estimates of abundance at RST sites and at Delta entry.

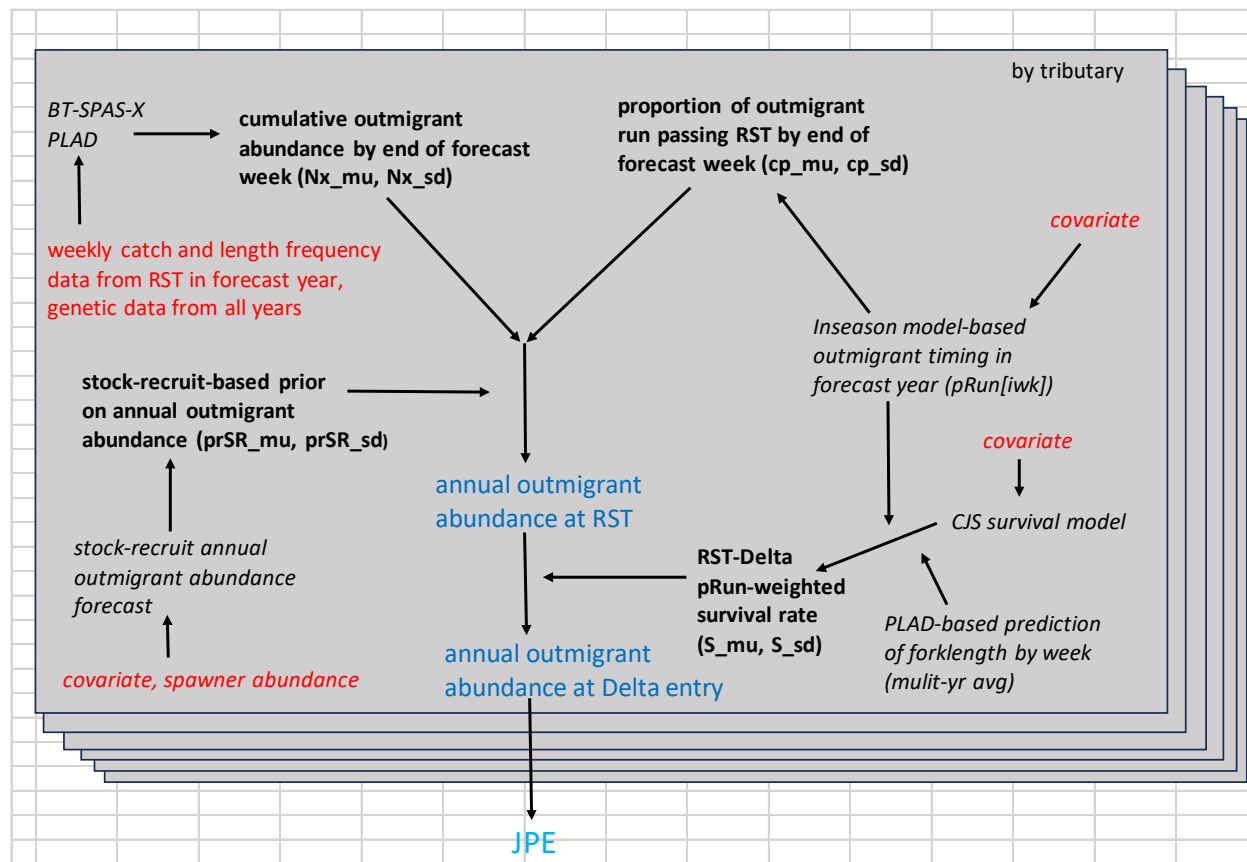


Figure 3. Stock-recruit Model Predicting Abundance at Deer Creek Rotary Screw Trap

Stock-recruit model predicting spring-run outmigrant annual abundance at the Deer Creek RSTs as a function of spawner abundance (adult holding counts) and the week in year when water temperature exceeds 13 C during the spawning and incubation period (si_above_13_temp_wk). Points show observations with labels identifying the brood year. The black line shows the median stock-recruit relationship at the average covariate condition across years. Vertical lines show predictions of outmigrant abundance for each brood year given its spawner abundance and covariate value. Blue lines indicate that the direction of the prediction, relative to predictions under the average covariate condition, (black line) is consistent with the observation, while red lines indicate the opposite. The dark gray shaded area shows the 80% credible interval at the average covariate condition due to uncertainty in stock-recruit parameters only. The light shaded area shows the 80% credible interval due to uncertainty in stock-recruit parameters and unexplained process error. The latter is used to quantify uncertainty for the prior on outmigration abundance at RST sites in srJPE.

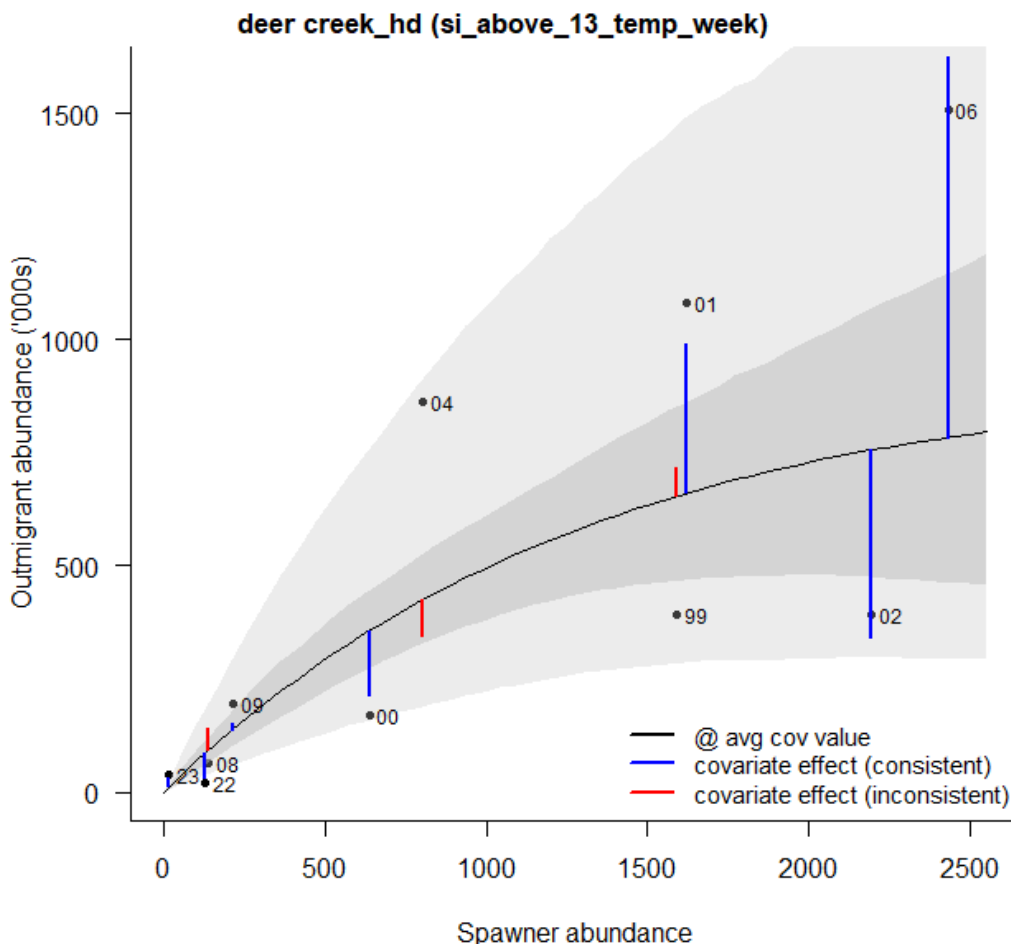


Figure 4. Forecasts of Spring-run Juvenile Outmigration Timing

Forecasts of spring-run juvenile outmigration timing for six Sacramento River tributaries with RSTs (Battle Creek, upper Clear Creek, Mill Creek, Deer Creek, Butte Creek, and Yuba River) and at two mainstem trapping sites (Tisdale and Knights Landing). The lines and shaded areas show the median and the 80% credible interval. Vertical lines identify the proportion of the outmigrant run passing the RSTs on the four forecast dates that were modeled. Note that mainstem outmigration timing predictions are not used in srJPE.

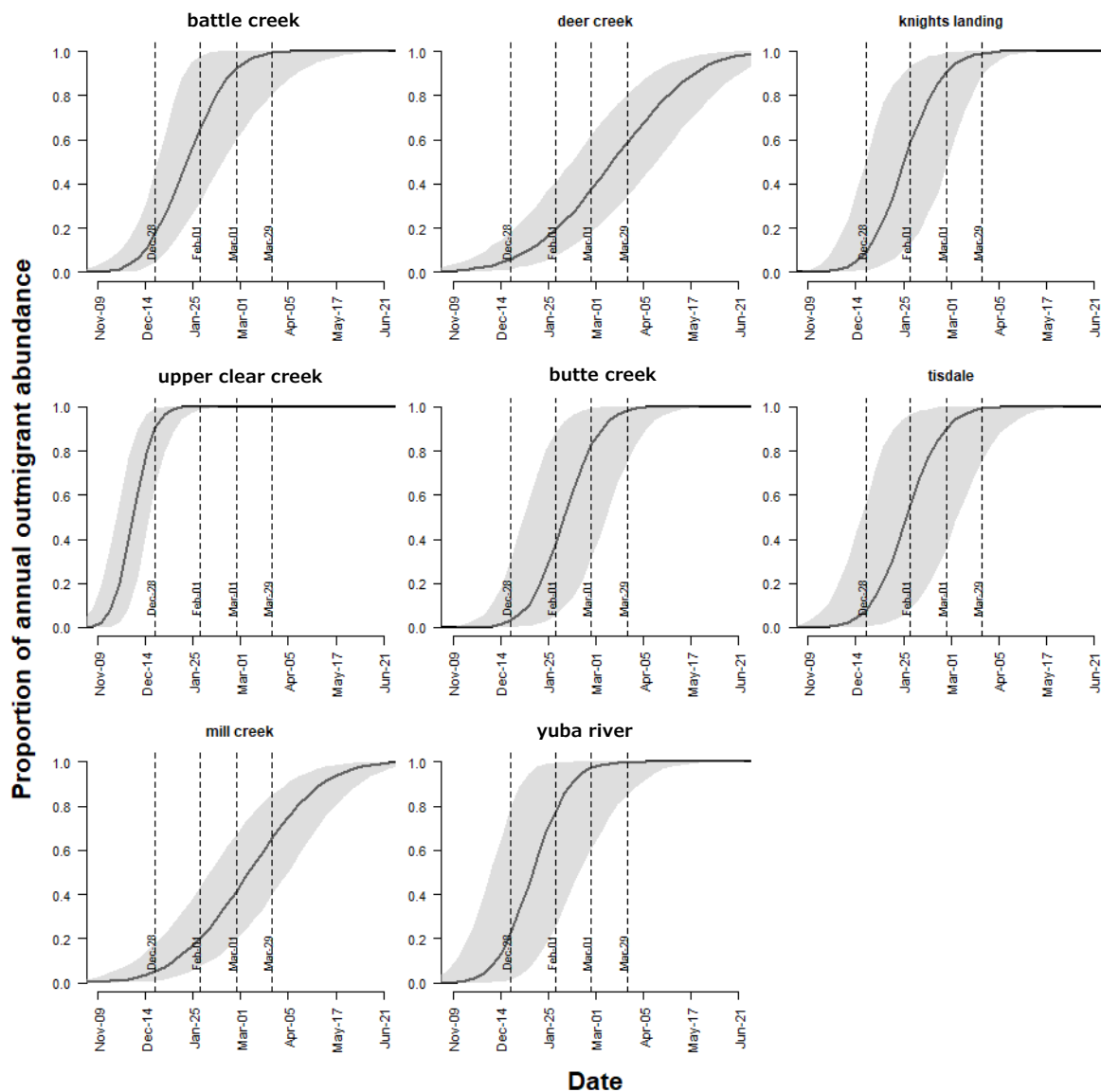


Figure 5. Predicted Weekly Abundance from Models at Upper Battle Creek Rotary Screw Trap in 2024

Predicted weekly abundance for juvenile Chinook salmon from the BT-SPAS-X model (all run types, top panel), the proportion of spring-run from the probabilistic length-at-date (PLAD) model (middle panel), and resulting abundance of spring-run abundance (bottom panel) at the upper Battle Creek RST in 2024. The bar height and error bars represent median values and 95% credible intervals, respectively. The titles for the top and bottom panels show the median, 95% credible interval (in parentheses), and the coefficient of variation (CV) of the annual outmigrant abundance estimates. The dashed vertical lines and arrows in the bottom panel show the weeks used to calculate cumulative abundance for each forecast week.

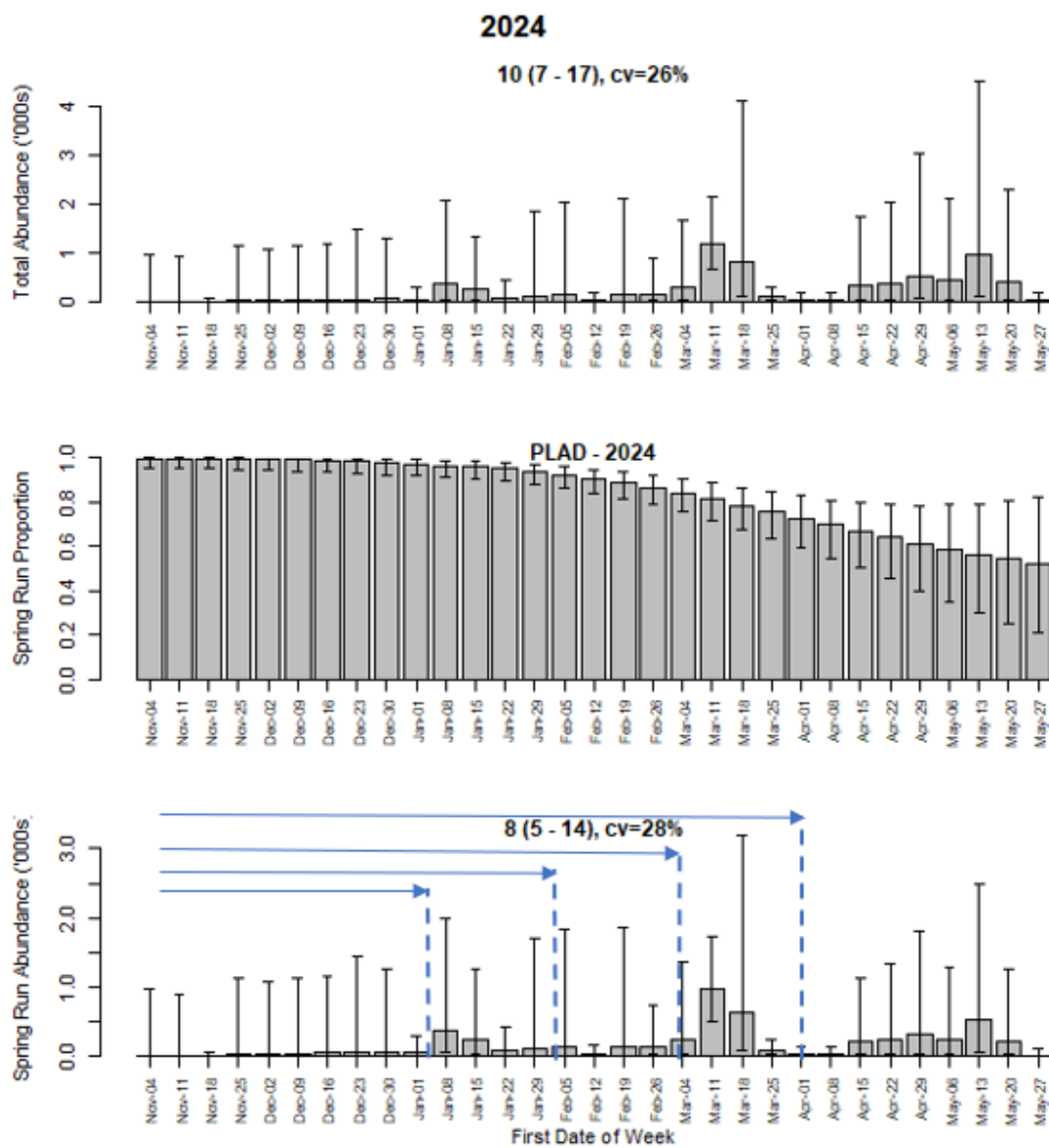


Figure 6. Predicted Survival Rate Estimated by Cormack-Jolly-Seber Submodel

Predicted survival rate from the release point of acoustically tagged Chinook salmon smolts to Delta entry as a function of fork length at release, estimated by the Cormack-Jolly-Seber (CJS) downstream survival submodel. The black sloped line shows the median relationship between fork length and survival, and the gray shaded area shows the 80% credible interval, noting that the relationships are extrapolated beyond the range of fish fork lengths used in acoustic tag survival studies. The vertical lines identify the average fork length of outmigrants calculated as a proportion-of-run weighted average of weekly predictions of fork length from the PLAD models: red = Mill, green = Deer, blue = Clear (masked by red line), black = Battle (masked by green line). Predictions are based on the average of peak flows during releases in the upper Sacramento River, Butte Creek, and Feather River. The title for each panel identifies the RST sites assigned to each relationship.

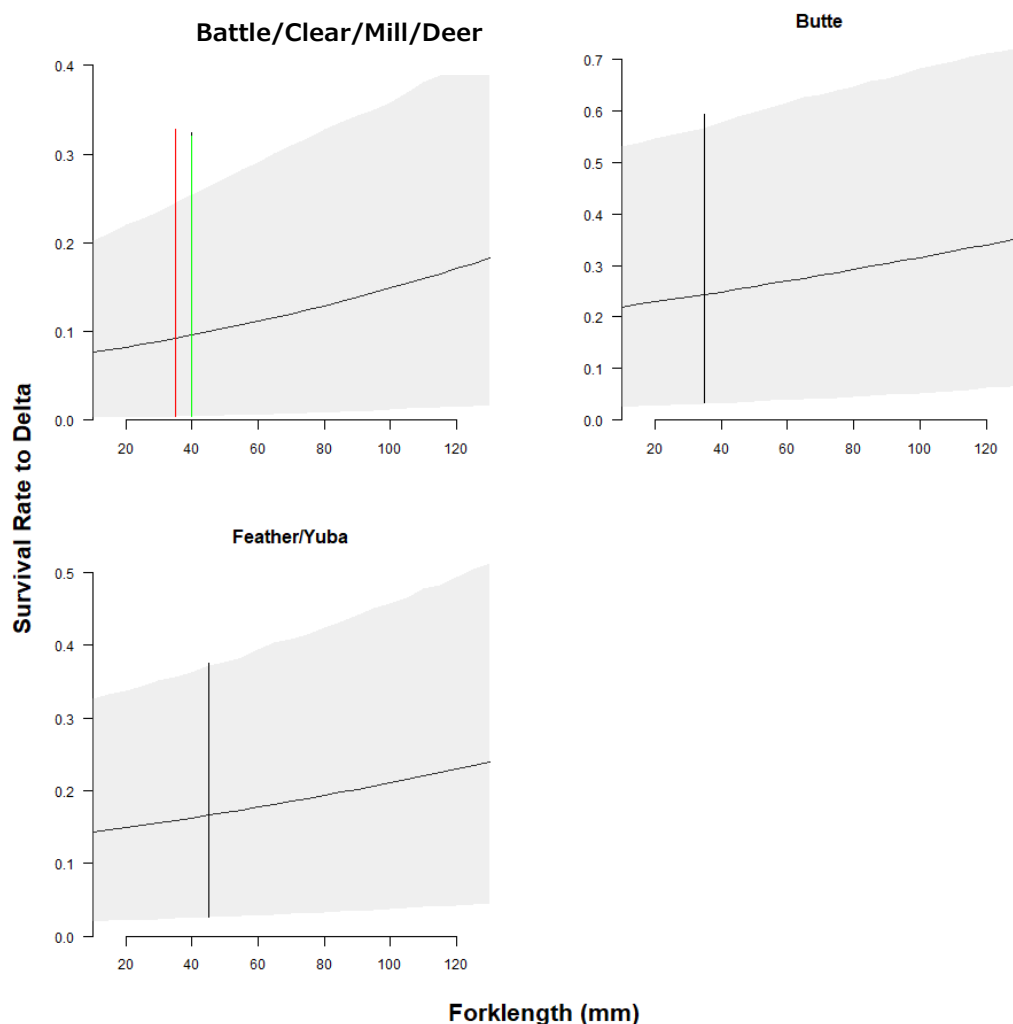


Figure 7. Predicted Survival Rate from Release Point to Delta Entry

Predicted survival rate from the release point of acoustically tagged Chinook salmon smolts to Delta entry as a function of peak flow during release for a 50-millimeter (mm) juvenile predicted by the CJS downstream survival model. Vertical lines show the assumed peak flows in the forecast year, which were set at the average values across all release groups for each system. Refer to the Figure 6 caption for additional details.

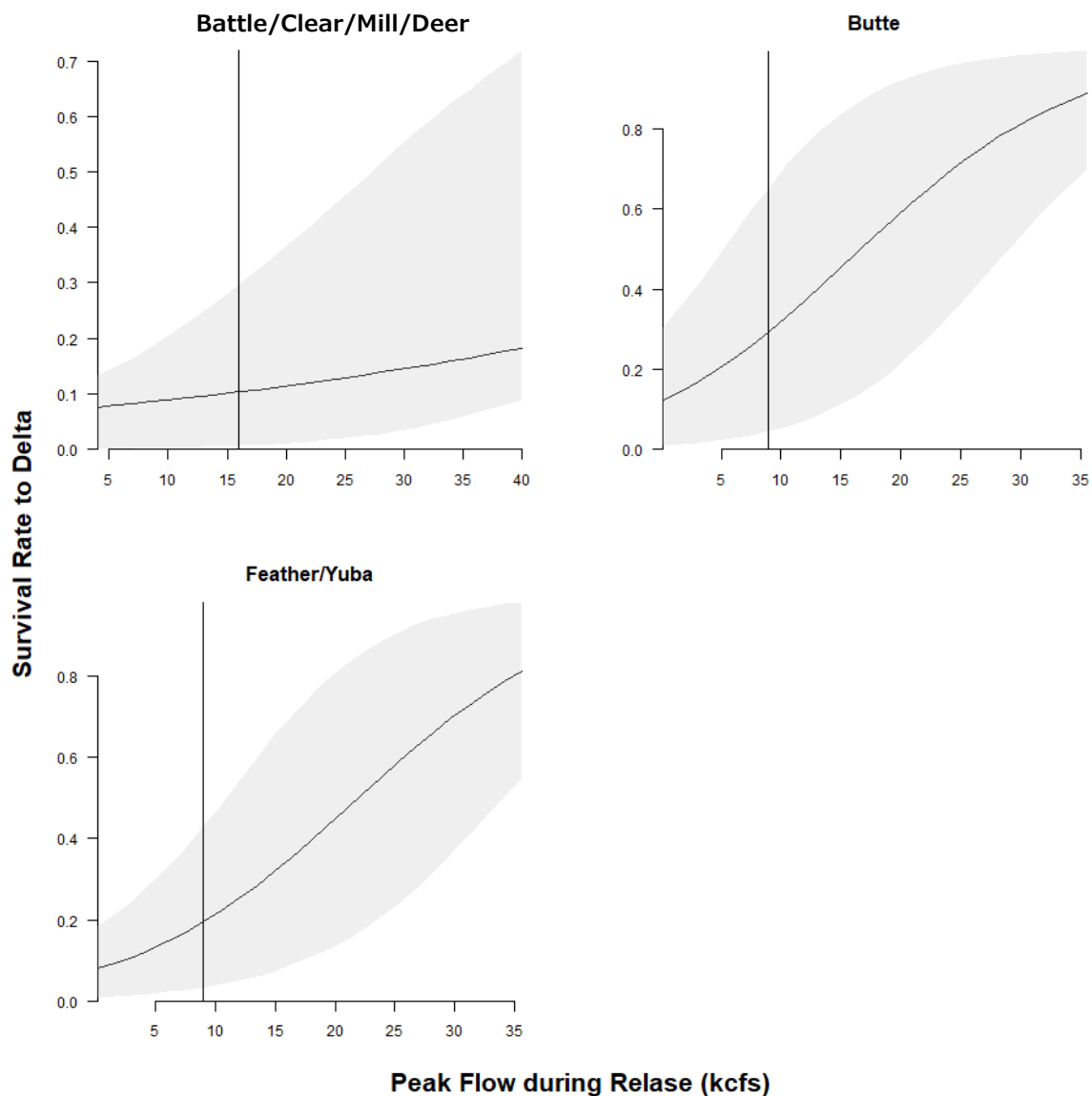


Figure 8. Outmigration Timing for Spring-run and Median Fork Length

Timing of outmigration for juvenile spring-run and median fork length at outmigration by week. The black line (y-axis on left) shows the median proportion of the annual abundance outmigrating by week as predicted by the inseason model. The red line (y-axis on right) shows the median fork length of outmigrants for each week as predicted by the PLAD model. The discontinuity of the date-fork length relationship occurs in the partial week at the end of the calendar year and is an artifact of data processing that will be removed in a future iteration of the modeling.

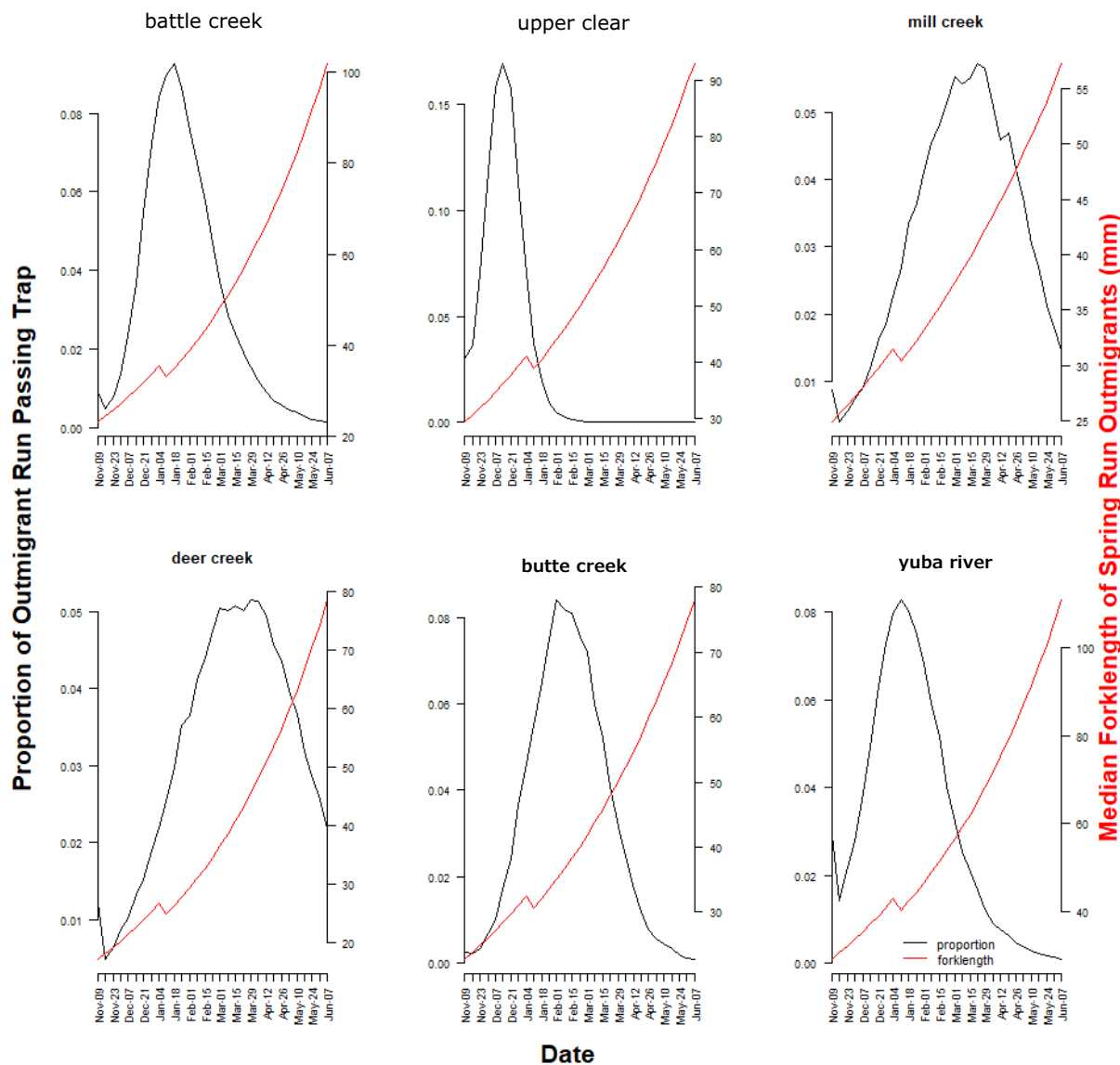


Figure 9. Median and 80% Credible Intervals of Survival Rate

Median and 80% credible intervals of the survival rate from RST sites to Delta entry used in srJPE. The forecast shown assumes that peak flows during outmigration were equal to the averages across release group from upper Sacramento (Battle, upper Clear, Mill, Deer creeks), Butte Creek and Yuba River.

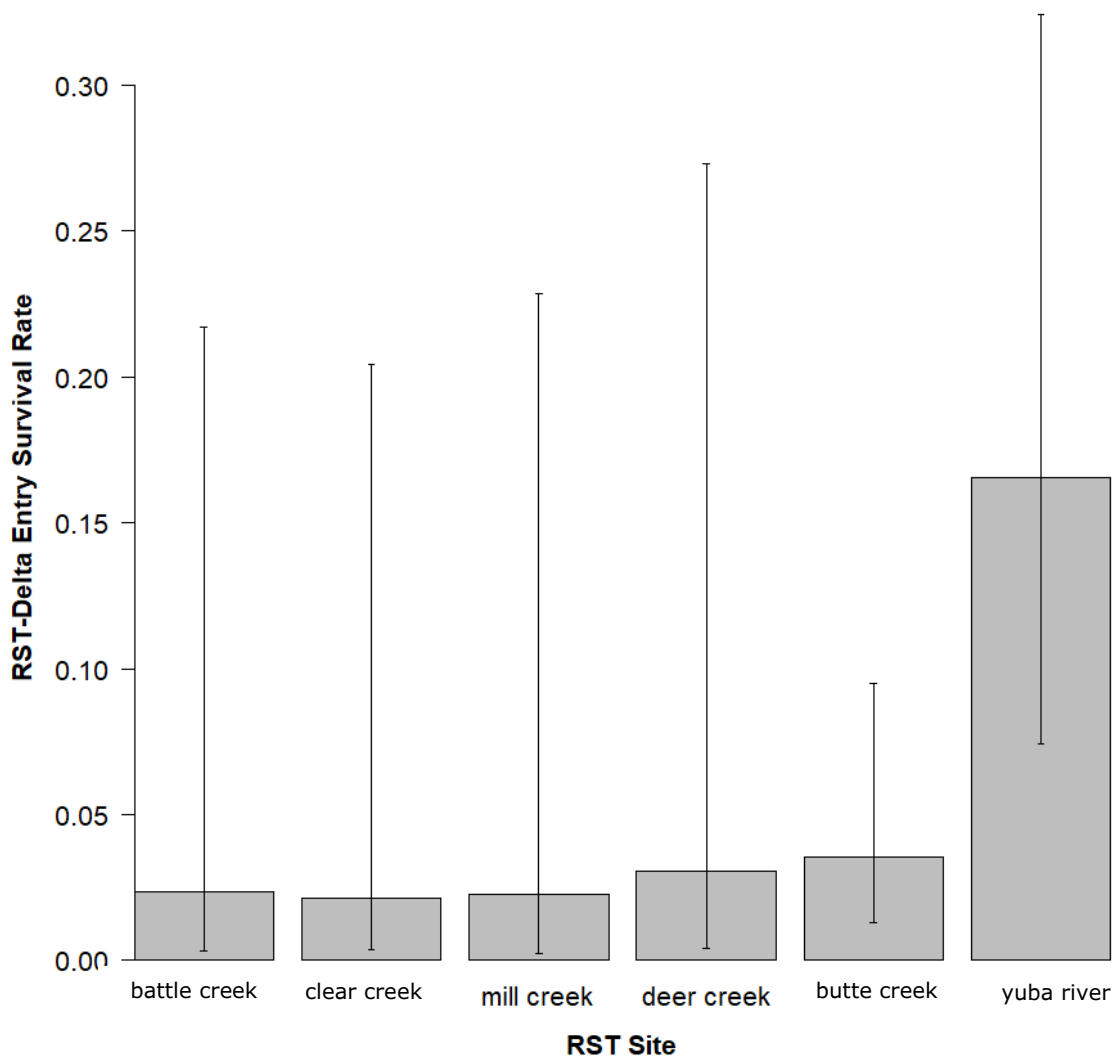


Figure 10. Structure of srJPE Predicting Timing of Spring-run Outmigrants

Structure of srJPE predicting the timing of spring-run Chinook salmon juvenile outmigrants at Delta entry. The graphic shows key output (blue text) and input (black bolded text) variables, supporting submodels (italics), and inputs to submodels in a forecast year (red text). Posterior distributions of weekly Delta arrival timing are estimated for each spring-run tributary with data, as denoted by the six tabs in the graphic (Battle, Clear, Mill, Deer, Butte creeks, Yuba River, and Feather River in the near future). These posteriors are combined to derive across-tributary aggregated arrival timing at Delta entry based on weighting factors that depend on forecasted abundance for each tributary (from stock-recruit submodel) and the average survival rate from RSTs to Delta entry (from CJS survival and travel time model).

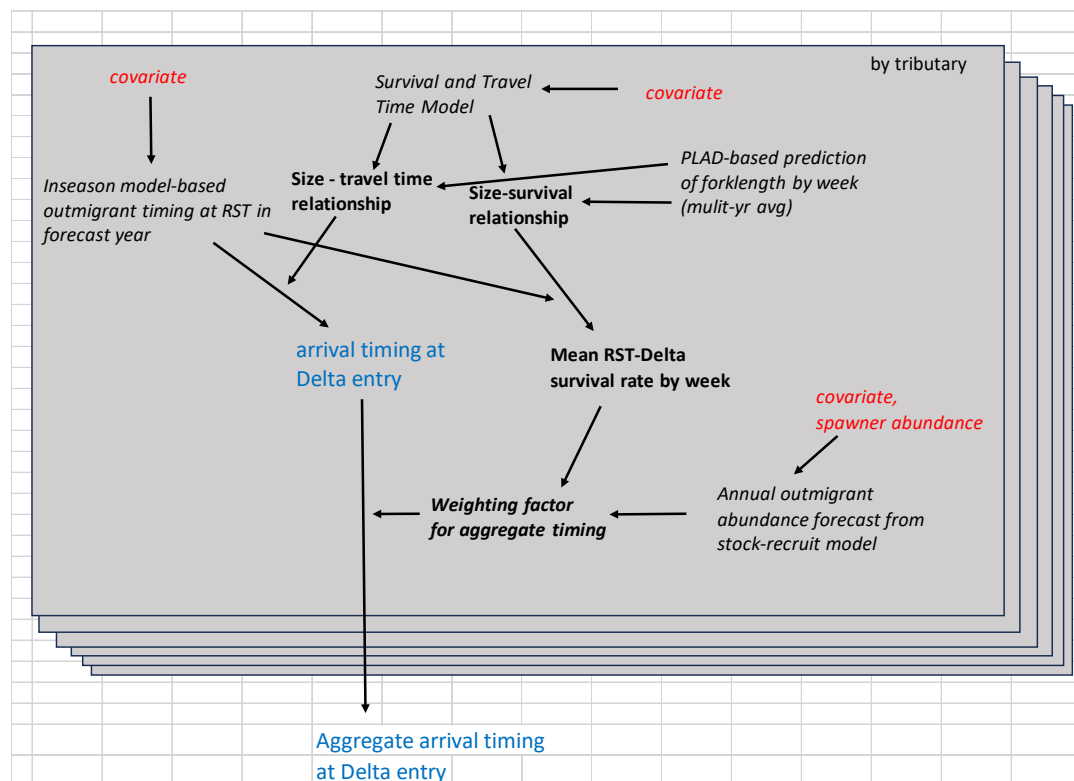


Figure 11. Forecast Travel Time as a Function of Monthly Peak Flows and Fork Length

Forecasted travel time from RST sites to the Delta as a function of monthly peak flows and fork length. The solid lines show median values and shaded areas show the 80% credible intervals. Estimates for panels in the top row are for an outmigrant with a fork length equal to the average among all acoustically tagged fish used to fit the travel time model (89 mm). Estimates for panels in the bottom row are calculated using the average of maximum monthly flows used to fit the travel time model (15.9 thousand cubic feet per second [kcfs] for upper Sacramento River sites, and 8.9 kcfs for tributaries).

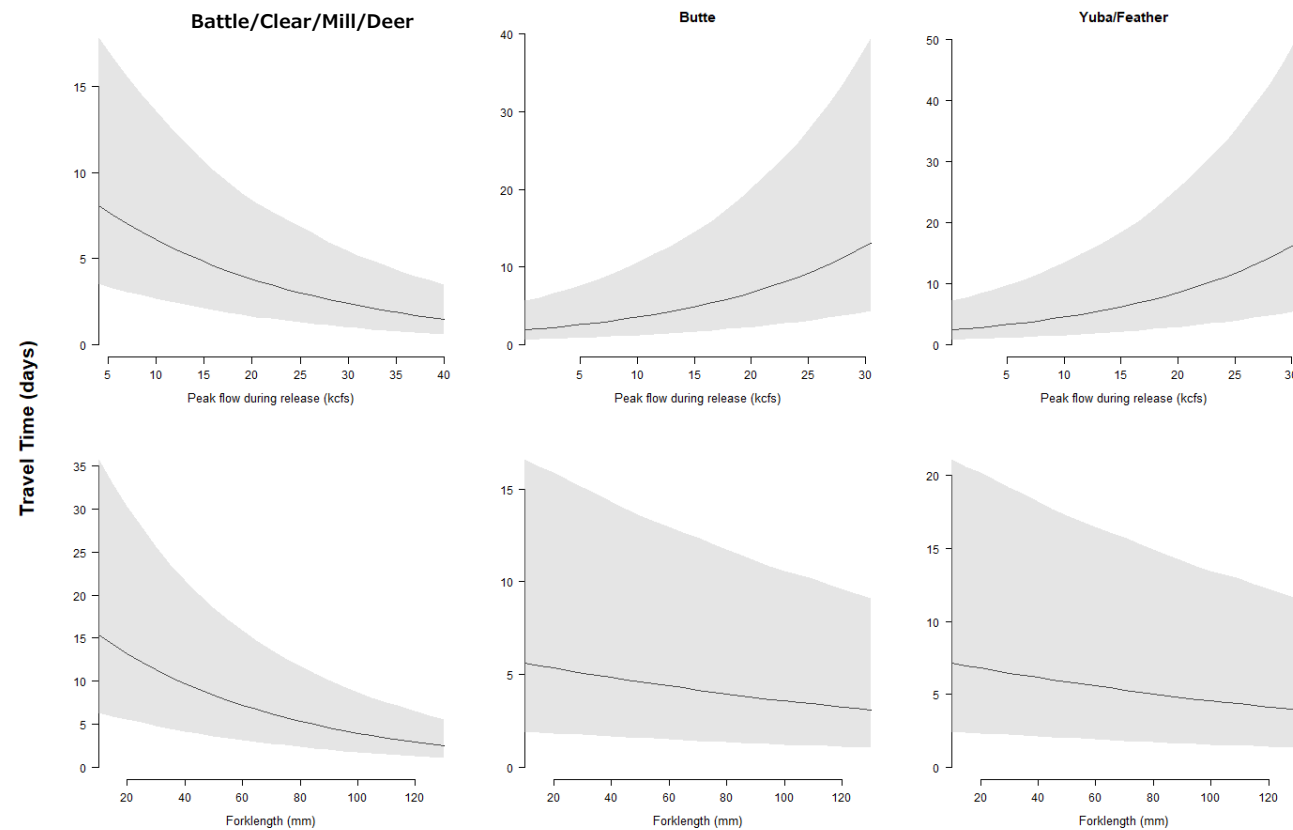


Figure 12. Forecast Travel Time from Rotary Screw Traps to Delta

Forecasted travel time from RSTs to Delta entry by model week. Travel times vary across weeks owing to changes in the mean fork length of outmigrants at the RSTs (refer to Figure 8). The solid lines show median values and shaded areas show the 80% credible intervals.

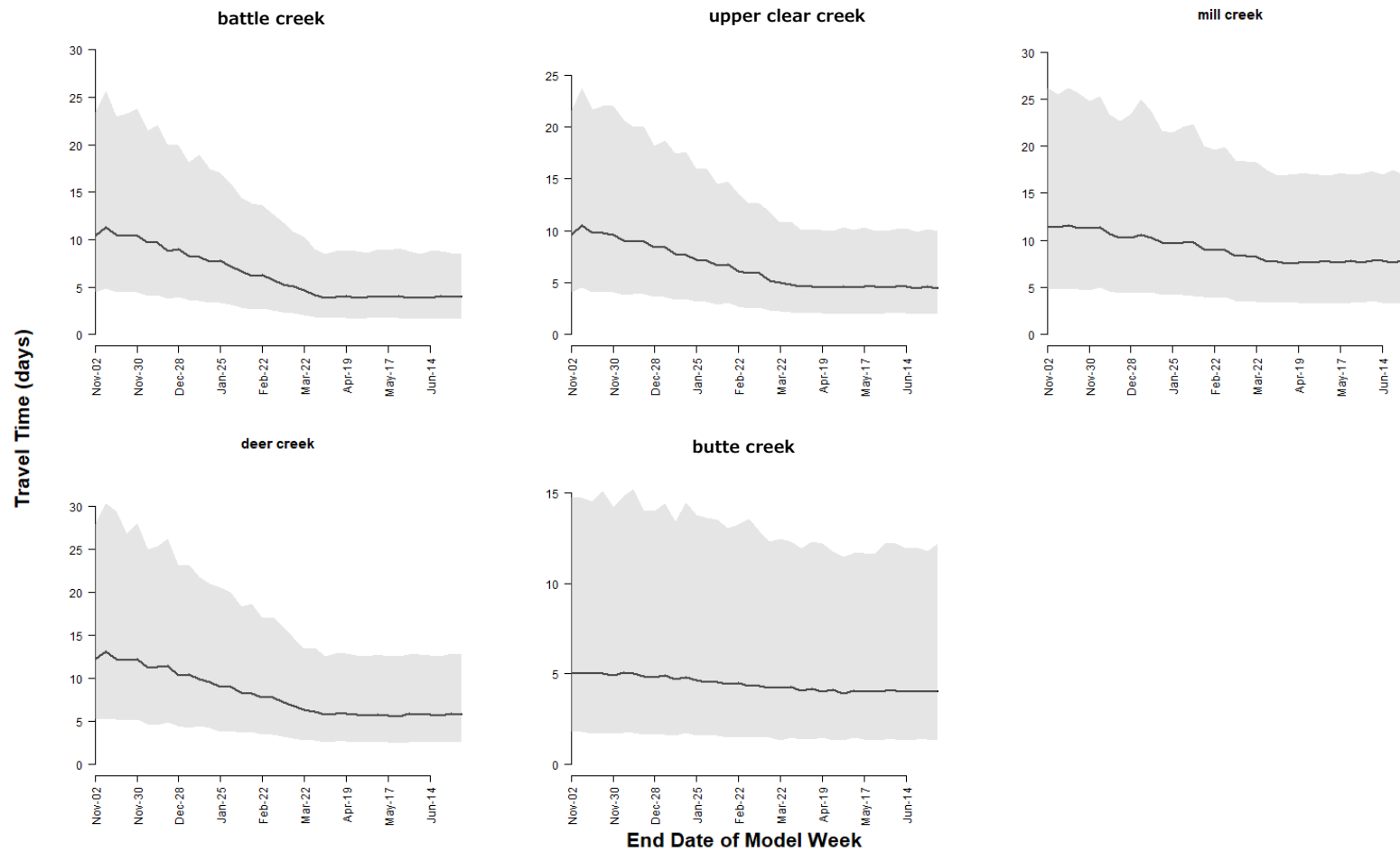


Figure 13. Forecast Survival Rate from Rotary Screw Traps to Delta Entry

Forecasted survival rate from RSTs to Delta entry by model week. Survival rate varies across weeks owing to changes in the mean fork length of outmigrants at the RSTs (refer to Figure 8). The solid lines show median values and shaded areas show the 80% credible intervals.

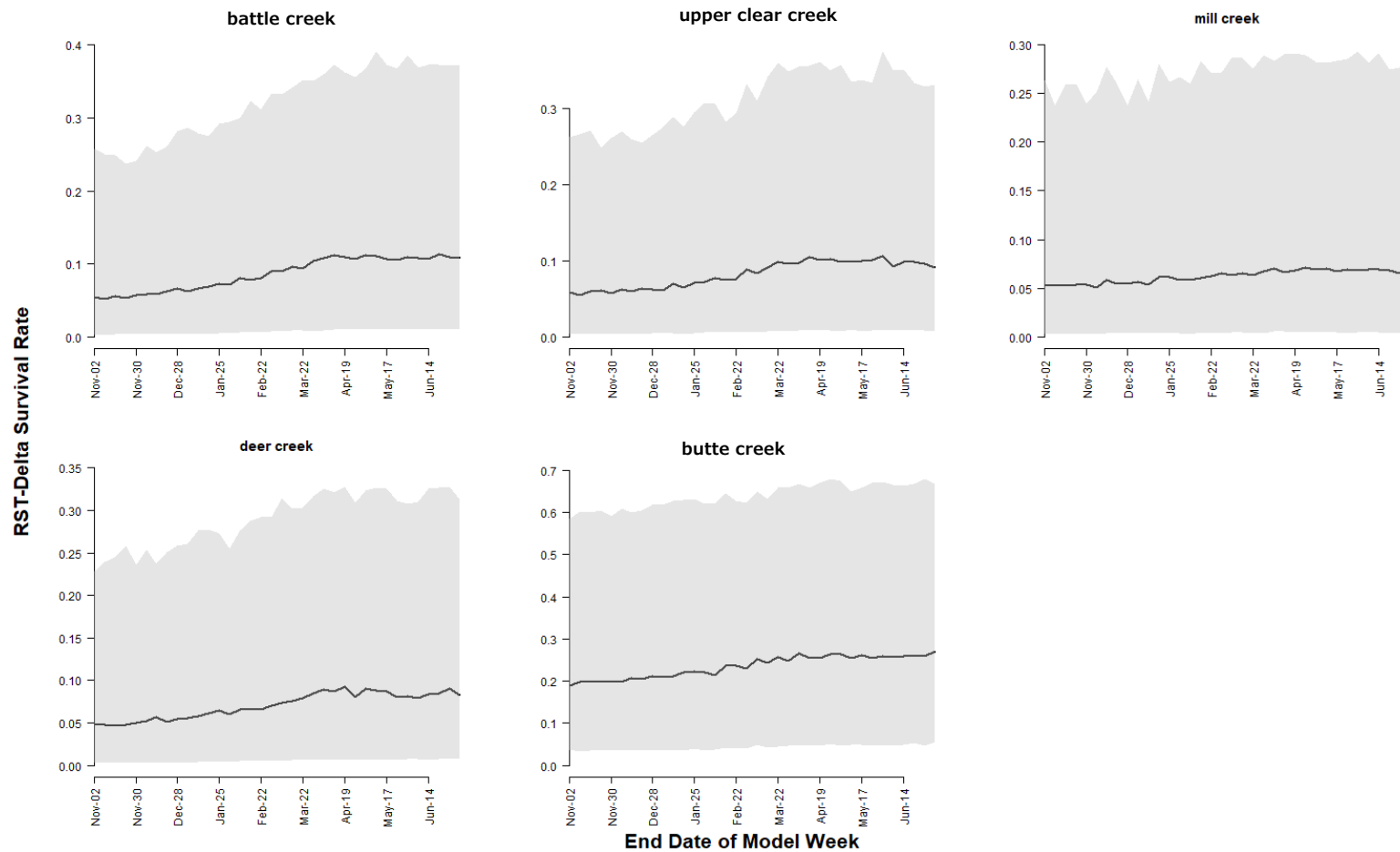


Figure 14. Summary of Prior and Posterior Distributions

Summary statistics of prior and posterior distributions to forecast spring-run annual juvenile abundance at RSTs in six tributaries of the Sacramento River. The height of bars and the red points show median values of posterior distributions. Error bars show 80% credible intervals. The bar labelled “SR” shows the forecast of annual outmigrant abundance from the stock-recruit submodel, which is used as a prior for abundance in srJPE. The other bars show the independent estimates of annual outmigrant abundance from the inseason model (refer to Equation 6) by forecast date. The red points and error bars show statistics of predicted annual abundance from srJPE.

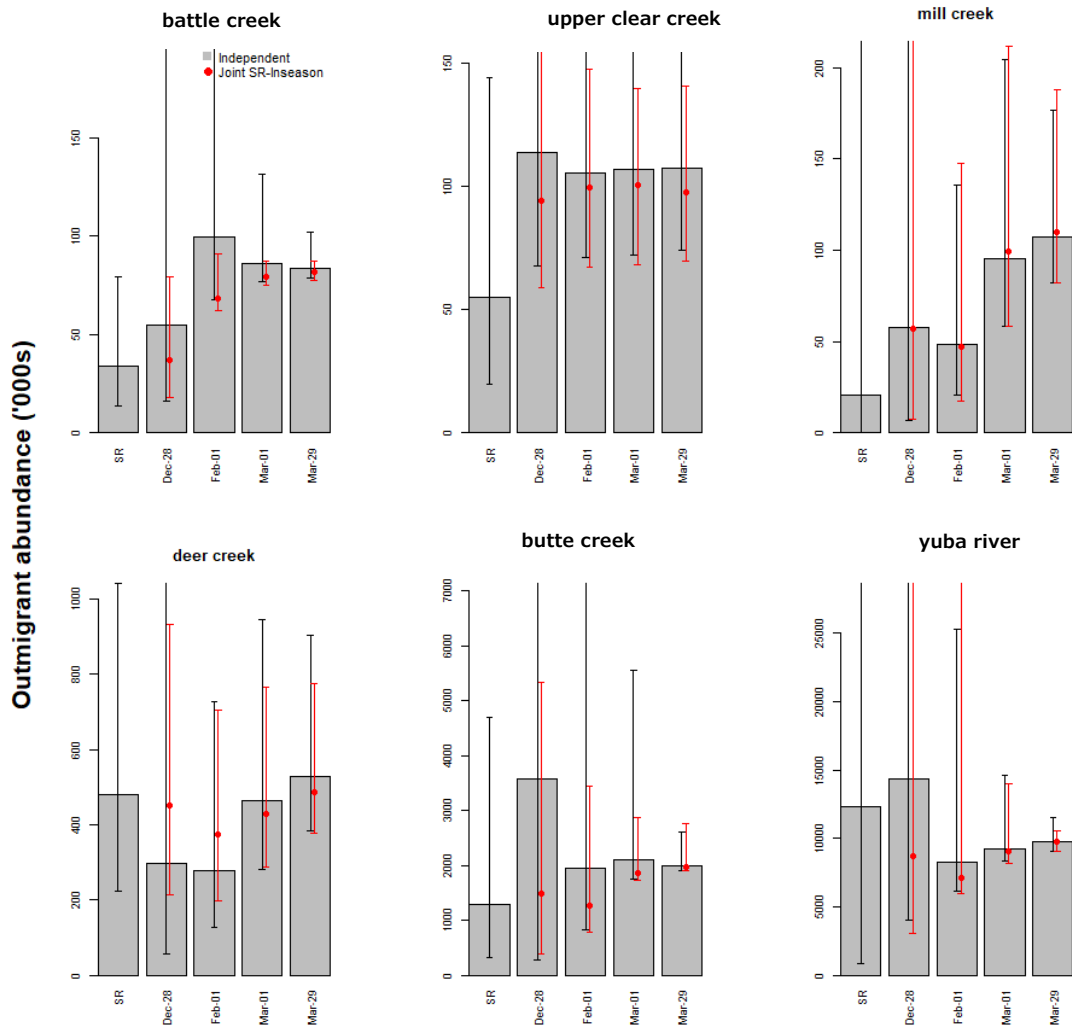


Figure 15. Comparison of Transformed Prior and Posterior Distributions from Integrated srJPE Model

Comparison of transformed prior (dashed line) and posterior (bars) distributions from srJPE by forecast date (columns). Results are shown for upper Battle (Figure 15a) and Mill (Figure 15b) creek RSTs. The top row shows the stock-recruit based prior (refer to Equation 1) and forecast of annual outmigrant abundance. The middle row shows the independent (refer to Equation 6) and posterior distributions (refer to Equation 5) of cumulative juvenile outmigrant abundance through each forecast week. The bottom row shows the independent (denominator of Equation 6) and posterior distributions (refer to Equation 4) of the cumulative proportion of outmigrants passing the RST site through each forecast week.

Figure 15a. Upper Battle Creek

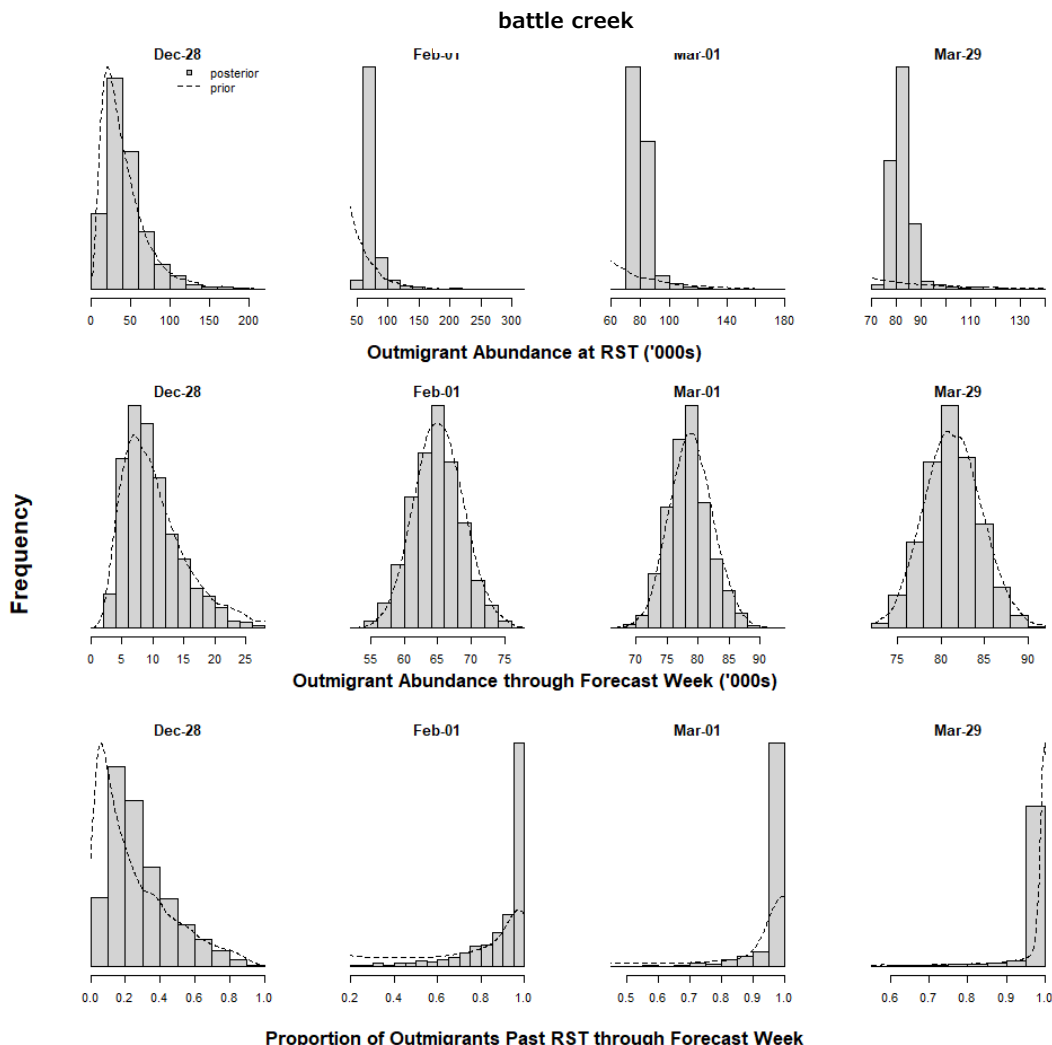


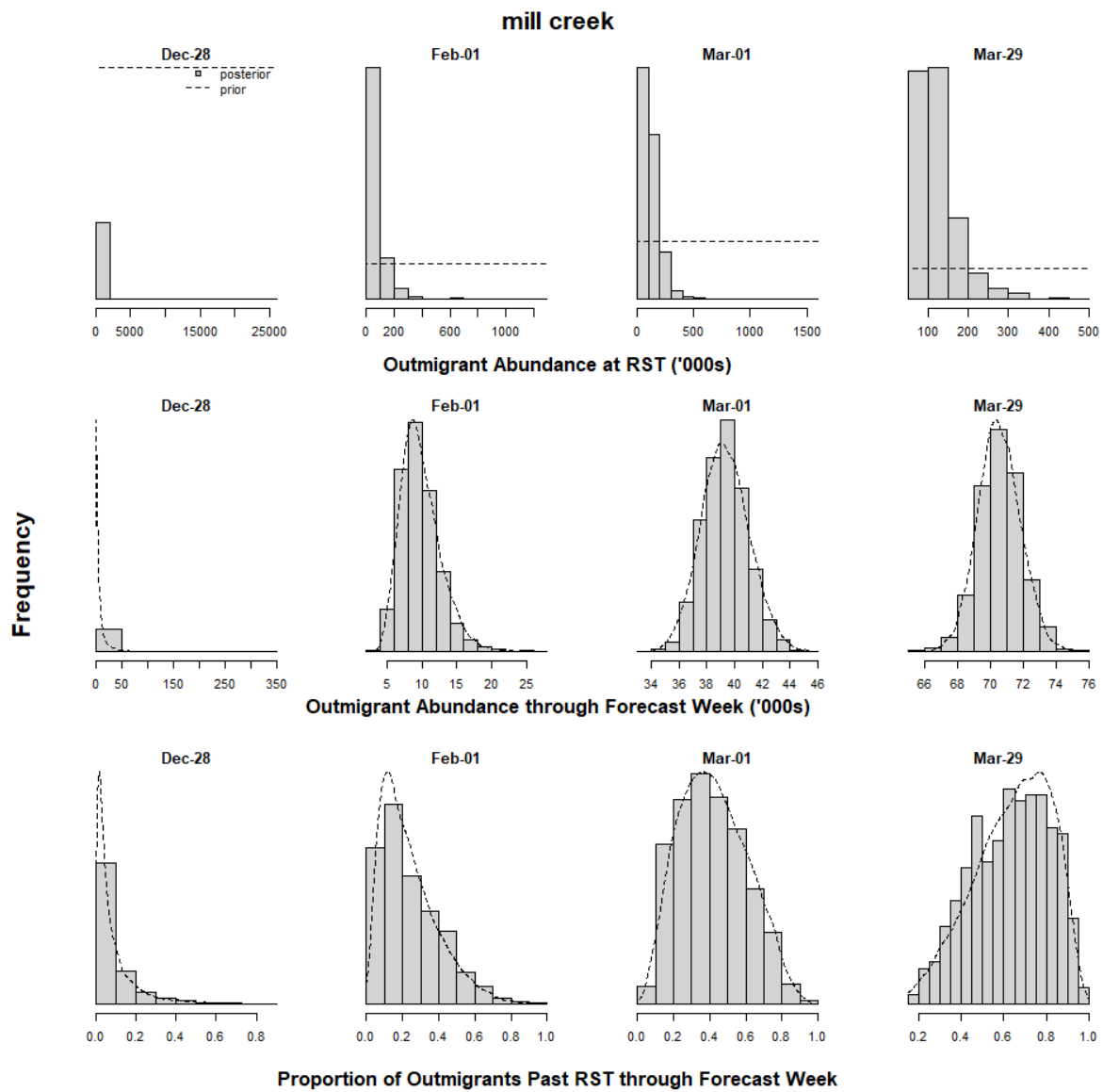
Figure 15b. Mill Creek

Figure 16. Integrated srJPE Model Predictions of Spring-run Abundance at Rotary Screw Trap Sites

Predictions of spring-run Chinook salmon juvenile abundance at RST sites summed across tributaries (red points, left y-axis) and abundance at Delta entry (blue points, right y-axis) by forecast date predicted by srJPE. Error bars show the lower 10% and upper 90% quantiles of the posterior distributions (i.e., the 80% credible intervals). Colored text identifies the 90% quantiles for cases that exceed the y-axis maxima.

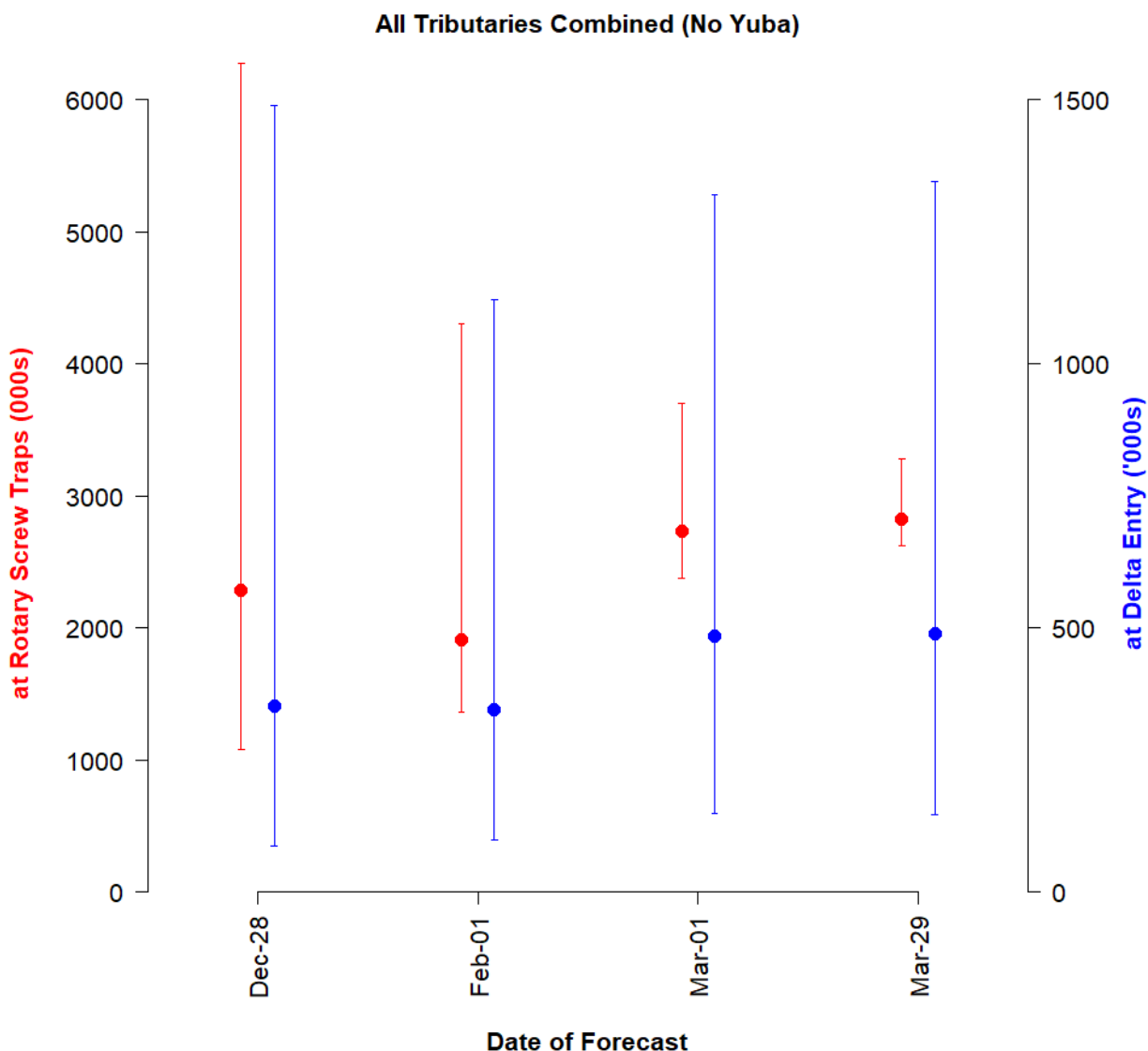


Figure 17. Pre-season Forecasts of Outmigration Timing at Rotary Screw Traps and at Delta Entry

Pre-season forecasts of juvenile outmigration timing at RSTs (black lines and gray shaded area) and at Delta entry (red lines and shaded area). The solid lines show median values and shaded areas show the 80% credible intervals. The title of each panel identifies the RST location and the product of the forecast of juvenile abundance in thousands of fish from the stock-recruit relationship. These abundances are used as part of the weighting factor to predict the aggregate timing relationships in the lower-right panel (i.e., the sum of timing across tributaries). Dashed lines identify the date when 50% of outmigrants have arrived at the Delta.

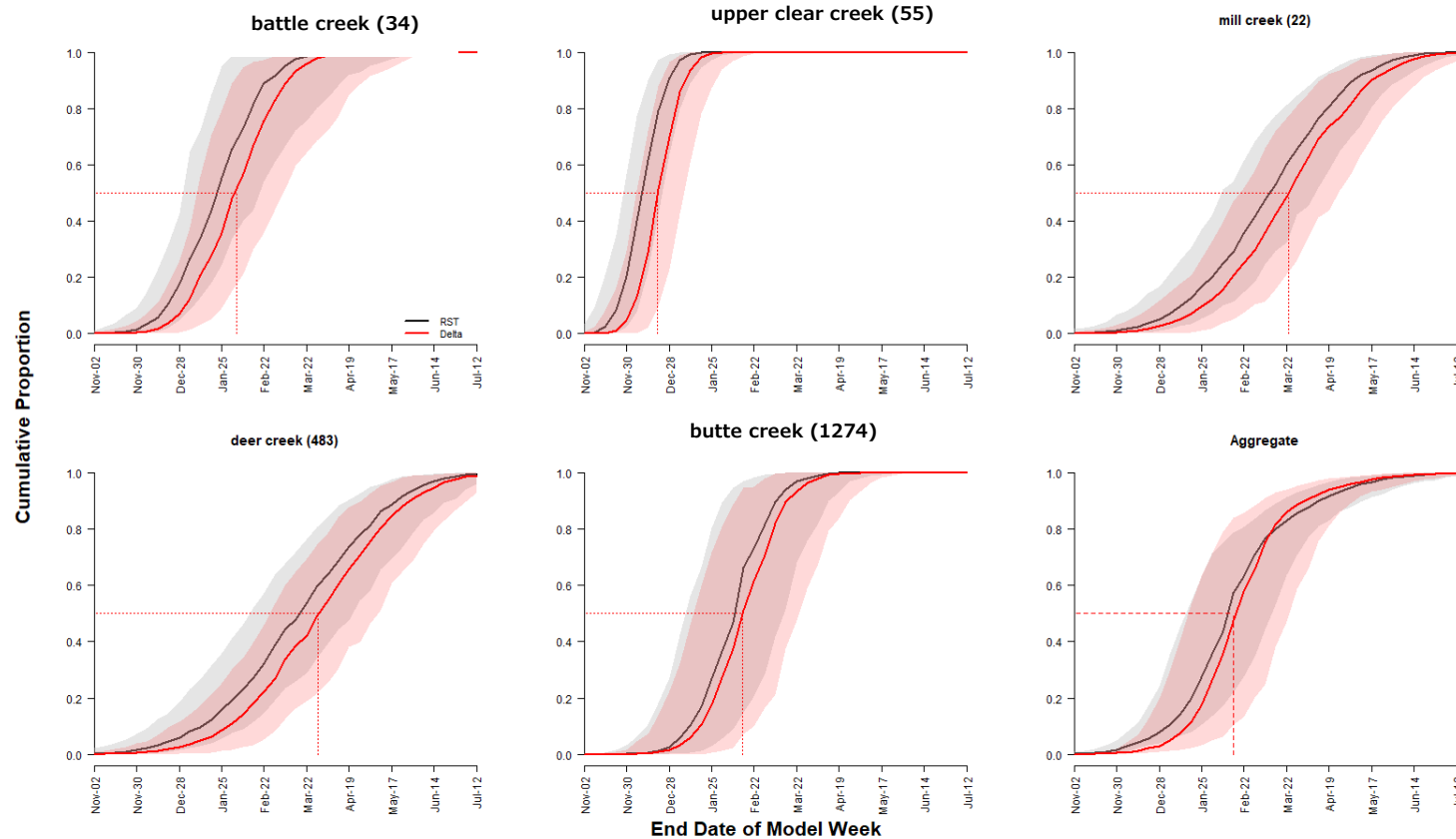


Figure 18. Pre-season Forecasts of Aggregate Juvenile Outmigration at Delta Entry

Pre-season forecasts of the aggregate (across-tributary) juvenile outmigration timing at Delta entry. The solid lines show median values and shaded areas show the 80% credible interval compared to forecasted timing from the inseason model for Tisdale (top) and Knights Landing (bottom) mainstem Sacramento River RSTs. Dashed lines identify the date when 50% of outmigrants have arrived at RST sites and the Delta.

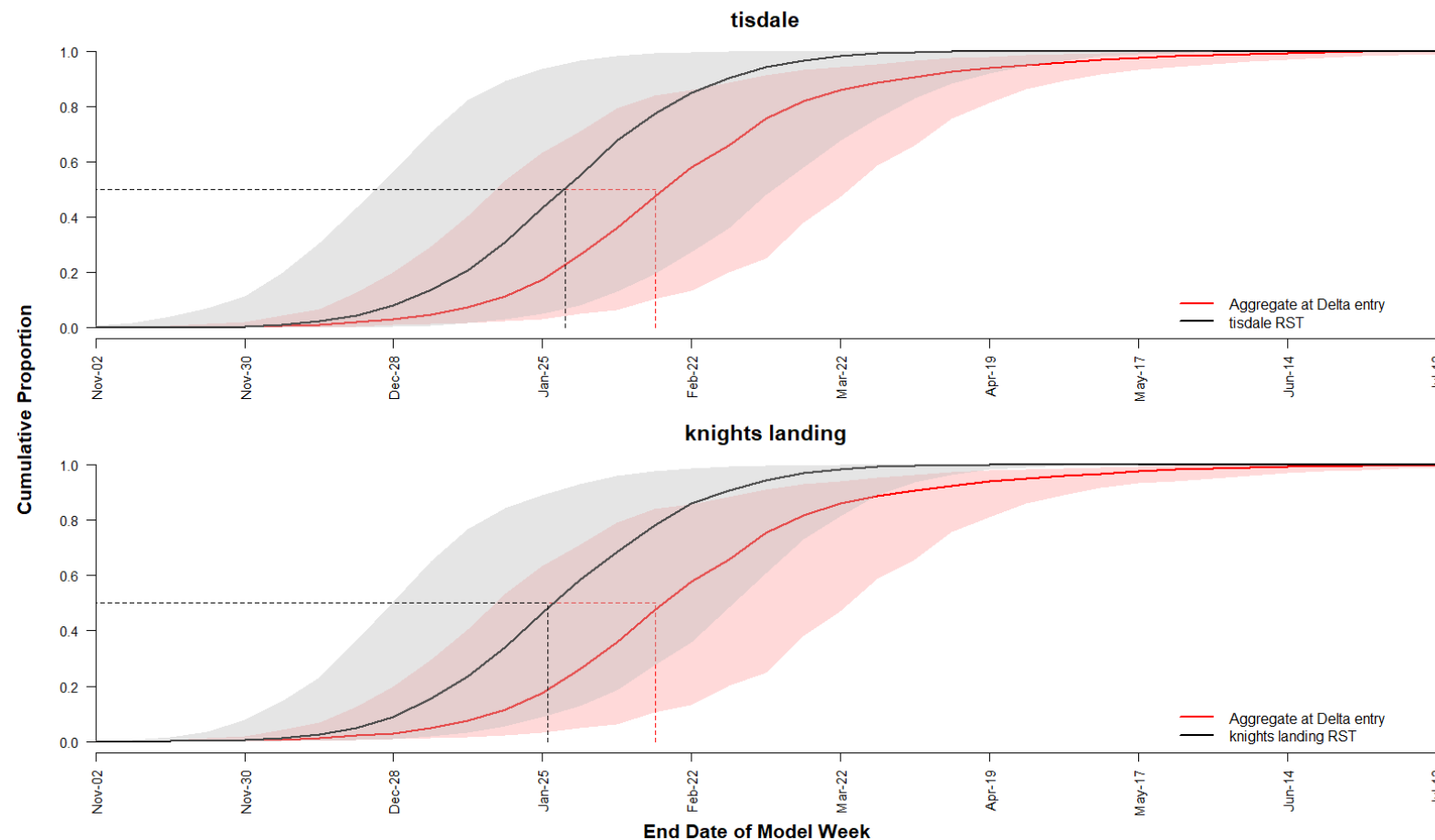
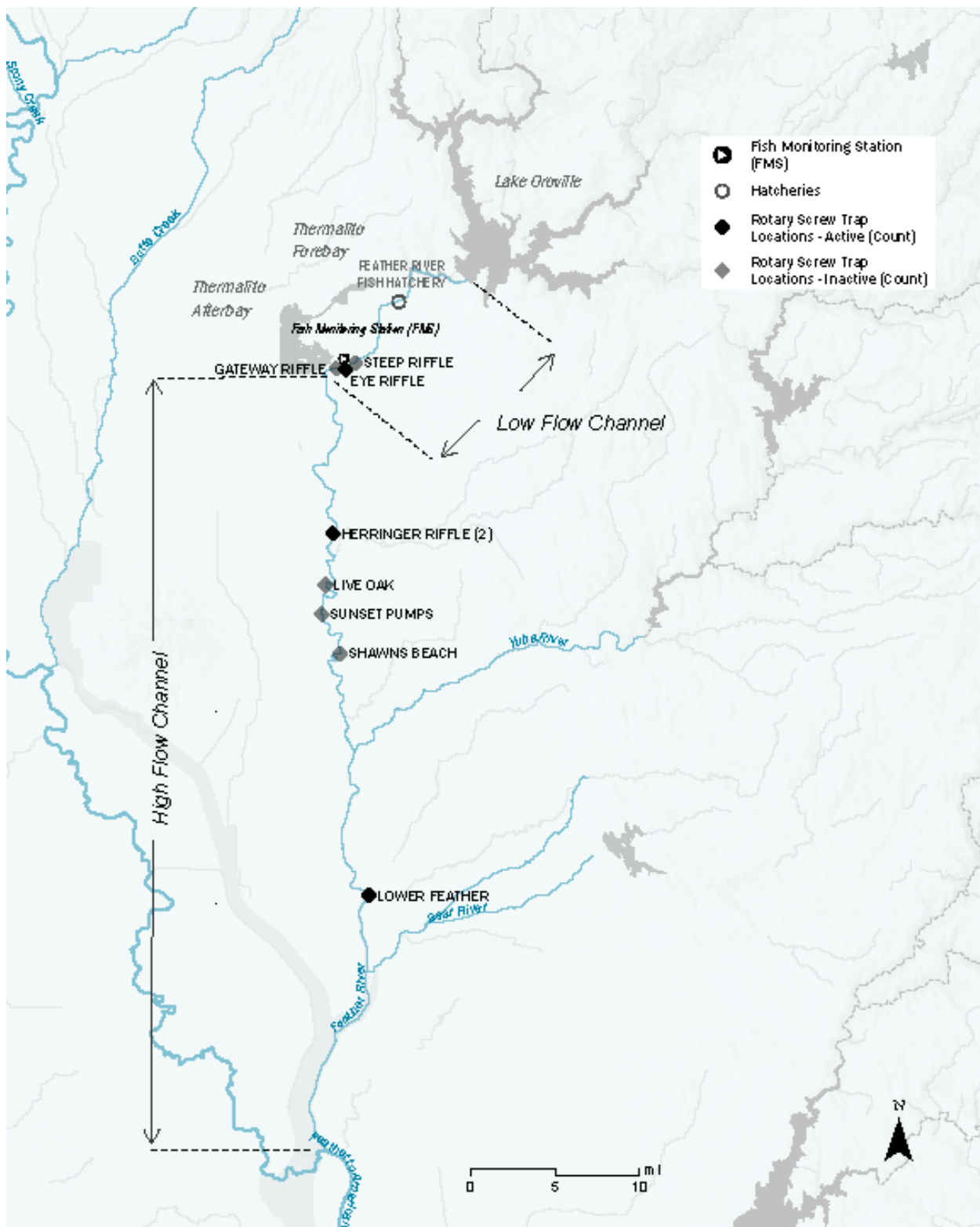


Figure 19. Feather River Map Showing Study Locations

Appendix

A. Integrated srJPE Model Source Code

```

data {
  int Ntribs;
  int Nfor;
  array[Ntribs,Nfor] real obs_Nx_mu; //mean of
  log cummulative abundance through each
  forecast week
  array[Ntribs,Nfor] real obs_Nx_sd; //sd of
  log cummulative abundance
  vector[Ntribs] srNtot_mu; //log of mean
  of abundance estimate from SR model that will
  be used as a prior
  vector[Ntribs] srNtot_sd; //log of sd of
  abundance estimate
  array[Ntribs,Nfor] real cp_mu; // mean of
  cumulative proportion of run passing by each
  forecast week in logit space from inseason
  model
  array[Ntribs,Nfor] real cp_sd; //sd of
  cumulative proportion
  vector[Ntribs] DS_surv_mu;//mean of weighted
  RST-Delta survival rate in logit sapace
  vector[Ntribs] DS_surv_sd;//sd
}

parameters {
  array[Ntribs,Nfor] real pred_lgNtot;
  //predicted annual abundance in log space
  array[Ntribs,Nfor] real lt_cp; //predicted
  cum prop past trap on forecast week in logit
  space
  array[Ntribs] real<lower=-6.5> lt_DS_surv;
  //survival to delta in logit space (can't be
  lower than ~ 0.15% survival)
}

transformed parameters{
  array[Ntribs,Nfor] real pred_lgNx;
  array[Ntribs,Nfor] real cp;
  for(itrib in 1:Ntribs){
    for(ifor in 1:Nfor){
      cp[itrib,ifor]=inv_logit(lt_cp[itrib,ifor]);/
      convert logit cp past trap
      pred_lgNx[itrib,ifor]=log(exp(pred_lgNtot[itr
      ib,ifor])*cp[itrib,ifor]);//predicted
      abundance on forecast wk is estimated annual
      abundance * cummulative proportion that has
      passed through that wk
    }
  }
}

model {//priors and data likelihood
  for(itrib in 1:Ntribs){
    for(ifor in 1:Nfor){
      obs_Nx_mu[itrib,ifor]~normal(pred_lgNx[itrib,
      ifor],obs_Nx_sd[itrib,ifor]);//'data'
      likelihood comparing 'observed' and predicted
      cum abundance through forecast week
      pred_lgNtot[itrib,ifor]~normal(srNtot_mu[itri
      b],srNtot_sd[itrib]);//prior on annual
      abundance from SR model
      lt_cp[itrib,ifor]~normal(cp_mu[itrib,ifor],cp
      _sd[itrib,ifor]);/// prior on cum proportion
      passing RST by forecast week in logit space
      from inseason model
    }
  }
}

generated quantities{
  array[Ntribs,Nfor] real pred_Ntot;
  array[Nfor] real pred_Ntot_all;
  array[Ntribs] real DS_surv;
  array[Ntribs,Nfor] real JPE_trib;
  array[Nfor] real JPE;
  for(itrib in 1:Ntribs){
    DS_surv[itrib]=inv_logit(lt_DS_surv[itrib]);/
    /RST to Delta-entry survival rate
  }
  for(ifor in 1:Nfor){
    for(itrib in 1:Ntribs){
      pred_Ntot[itrib,ifor]=exp(pred_lgNtot[itrib,i
      for]);//convert annual abundance estimate
      from log space
      JPE_trib[itrib,ifor]=pred_Ntot[itrib,ifor]*DS
      _surv[itrib];//predict abundance at Delta
      entry
    }
  }
  pred_Ntot_all[ifor]=sum(pred_Ntot[1:Ntribs,i
  for]);//outmigrant abundance at RST summed
  across tributaries
  JPE[ifor]=sum(JPE_trib[1:Ntribs,ifor]);//outm
  igrant abundance at delta entry summed across
  tribs.
}
}

```